Neurobiology of Disease 182 (2023) 106140

Contents lists available at ScienceDirect

Neurobiology of Disease

journal homepage: www.elsevier.com/locate/ynbdi

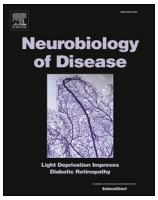

Protective Alzheimer's disease-associated APP A673T variant predominantly decreases sAPPβ levels in cerebrospinal fluid and 2D/3D cell culture models

Rebekka Wittrahm [a], Mari Takalo [a], Teemu Kuulasmaa [a], Petra M. Mäkinen [a], Petri Mäkinen [b], Saša Končarević [c], Vadim Fartzdinov [c], Stefan Selzer [c], Tarja Kokkola [d], Leila Antikainen [d], Henna Martiskainen [a], Susanna Kemppainen [a], Mikael Marttinen [e,f], Heli Jeskanen [a], Hannah Rostalski [b], Eija Rahunen [a], Miia Kivipelto [g,h,i,j,k], Tiia Ngandu [g,h], Teemu Natunen [a], Jean-Charles Lambert [l], Rudolph E. Tanzi [m], Doo Yeon Kim [m], Tuomas Rauramaa [n,o], Sanna-Kaisa Herukka [p,q], Hilkka Soininen [p], Markku Laakso [d,r], Ian Pike [s], Ville Leinonen [t], Annakaisa Haapasalo [b], Mikko Hiltunen [a,*]

[a] Institute of Biomedicine, University of Eastern Finland, 70211 Kuopio, Finland
[b] A.I. Virtanen Institute for Molecular Sciences, 70211 Kuopio, Finland
[c] Proteome Sciences GmbH & Co. KG, 60438 Frankfurt, Germany
[d] Institute of Clinical Medicine, Internal Medicine, University of Eastern Finland, 70210 Kuopio, Finland
[e] Faculty of Medicine and Health Technology, Tampere University, 33520 Tampere, Finland
[f] Structural and Computational Biology Unit, European Molecular Biology Laboratory, 69117 Heidelberg, Germany
[g] Population Health Unit, Finnish Institute for Health and Welfare, Helsinki, Finland
[h] Division of Clinical Geriatrics, Department of Neurobiology, Center for Alzheimer Research, Care Sciences and Society, Karolinska Institutet, Stockholm, Sweden
[i] The Ageing Epidemiology Research Unit, School of Public Health, Imperial College London, London, United Kingdom
[j] Theme Aging, Karolinska University Hospital, Stockholm, Sweden
[k] Institute of Public Health and Clinical Nutrition, University of Eastern Finland, 70211 Kuopio, Finland
[l] U1167, University of Lille, Inserm, Institut Pasteur de Lille, F-59000 Lille, France
[m] Genetics and Aging Research Unit, McCance Center for Brain Health, MassGeneral Institute for Neurodegenerative Disease, Department of Neurology, Massachusetts General Hospital and Harvard Medical School, Boston, MA, United States
[n] Department of Pathology, Kuopio University Hospital, 70211 Kuopio, Finland
[o] Unit of Pathology, Institute of Clinical Medicine, University of Eastern Finland, 70210 Kuopio, Finland
[p] Department of Neurology, University of Eastern Finland, 70210 Kuopio, Finland
[q] NeuroCenter, Neurology, Kuopio University Hospital, Kuopio, Finland
[r] Department of Medicine, Kuopio University Hospital, 70210 Kuopio, Finland
[s] Proteome Sciences plc, Hamilton House, London, WC1H 9BB, UK
[t] Department of Neurosurgery, Kuopio University Hospital, and Institute of Clinical Medicine, Unit of Neurosurgery, University of Eastern Finland, Kuopio, Finland

ARTICLE INFO

Keywords:
Alzheimer's disease
APP A673T variant
Cerebrospinal fluid

ABSTRACT

The rare A673T variant was the first variant found within the amyloid precursor protein (APP) gene conferring protection against Alzheimer's disease (AD). Thereafter, different studies have discovered that the carriers of the APP A673T variant show reduced levels of amyloid beta (Aβ) in the plasma and better cognitive performance at high age. Here, we analyzed cerebrospinal fluid (CSF) and plasma of APP A673T carriers and control individuals

* Corresponding author.
E-mail addresses: rebekka.wittrahm@uef.fi (R. Wittrahm), mari.takalo@uef.fi (M. Takalo), teemu.kuulasmaa@uef.fi (T. Kuulasmaa), petra.makinen@uef.fi (P.M. Mäkinen), petri.makinen@uef.fi (P. Mäkinen), sasa.koncarevic@proteomics.com (S. Končarević), stefan.selzer@proteomics.com (S. Selzer), tarja.kokkola@uef.fi (T. Kokkola), leila.antikainen@uef.fi (L. Antikainen), henna.martiskainen@uef.fi (H. Martiskainen), susanna.kemppainen@uef.fi (S. Kemppainen), mikael.marttinen@tuni.fi (M. Marttinen), heli.jeskanen@uef.fi (H. Jeskanen), hannah.rostalski@uef.fi (H. Rostalski), eija.rahunen@uef.fi (E. Rahunen), miia.kivipelto@ki.se (M. Kivipelto), teemu.natunen@uef.fi (T. Natunen), jean-charles.lambert@pasteur-lille.fr (J.-C. Lambert), tanzi@helix.mgh.harvard.edu (R.E. Tanzi), dkim@helix.mgh.harvard.edu (D.Y. Kim), tuomas.rauramaa@kuh.fi (T. Rauramaa), sanna-kaisa.herukka@uef.fi (S.-K. Herukka), hilkka.soininen@uef.fi (H. Soininen), markku.laakso@uef.fi (M. Laakso), ian.pike@proteomics.com (I. Pike), ville.leinonen@kuh.fi (V. Leinonen), annakaisa.haapasalo@uef.fi (A. Haapasalo), mikko.hiltunen@uef.fi (M. Hiltunen).

https://doi.org/10.1016/j.nbd.2023.106140
Received 23 February 2023; Received in revised form 23 April 2023; Accepted 25 April 2023
Available online 28 April 2023

Protective mechanisms
2D/3D cell models

using a mass spectrometry-based proteomics approach to identify differentially regulated targets in an unbiased manner. Furthermore, the APP A673T variant was introduced into 2D and 3D neuronal cell culture models together with the pathogenic APP Swedish and London mutations. Consequently, we now report for the first time the protective effects of the APP A673T variant against AD-related alterations in the CSF, plasma, and brain biopsy samples from the frontal cortex. The CSF levels of soluble APPβ (sAPPβ) and Aβ42 were significantly decreased on average 9–26% among three APP A673T carriers as compared to three well-matched controls not carrying the protective variant. Consistent with these CSF findings, immunohistochemical assessment of cortical biopsy samples from the same APP A673T carriers did not reveal Aβ, phospho-tau, or p62 pathologies. We identified differentially regulated targets involved in protein phosphorylation, inflammation, and mitochondrial function in the CSF and plasma samples of APP A673T carriers. Some of the identified targets showed inverse levels in AD brain tissue with respect to increased AD-associated neurofibrillary pathology. In 2D and 3D neuronal cell culture models expressing APP with the Swedish and London mutations, the introduction of the APP A673T variant resulted in lower sAPPβ levels. Concomitantly, the levels of sAPPα were increased, while decreased levels of CTFβ and Aβ42 were detected in some of these models. Our findings emphasize the important role of APP-derived peptides in the pathogenesis of AD and demonstrate the effectiveness of the protective APP A673T variant to shift APP processing towards the non-amyloidogenic pathway in vitro even in the presence of two pathogenic mutations.

1. Introduction

Alzheimer's disease (AD) is a progressive neurodegenerative disorder and the most common cause of dementia. The disease is characterized by extracellular amyloid plaques, intracellular neurofibrillary tangles (NFT), composed of hyperphosphorylated tau protein, and neuronal loss (Shankar and Walsh, 2009; Hardy and Allsop, 1991; Goedert et al., 1991). Amyloid plaques emerge from the accumulation of β-amyloid (Aβ), which are derived from amyloid precursor protein (APP) via amyloidogenic processing through sequential cleavage by the β- and γ-secretases (Selkoe, 1998). When APP is subjected to β-secretase cleavage, β-C-terminal fragment (CTFβ) and soluble APPβ (sAPPβ) are generated. Further processing of CTFβ by γ-secretase then leads to the production of Aβ peptides of different lengths (Xu, 2009). While Aβ40 is the predominant Aβ isoform in the healthy brain, Aβ42 has been shown to be more prone to form aggregates, which exhibit higher toxicity than Aβ40 aggregates (Bernstein et al., 2009). Aβ42 is the earliest clinical biomarker indicative of AD that changes in CSF and plasma samples, followed by an increase in the level of phosphorylated tau (p-tau) (Palmqvist et al., 2019). In the usually predominant non-amyloidogenic pathway, APP is cleaved within the Aβ sequence by α-secretase into an α-C-terminal fragment (CTFα) and soluble APPα (sAPPα) peptide.

AD is a multifactorial disorder with a high degree of heritability (Gatz et al., 2006; Ridge et al., 2013). Only<1% of AD cases are accounted for by autosomal dominant causative genetic variants identified within *APP* and γ-secretase subunit presenilin1 (*PSEN1*), or presenilin2 (*PSEN2*) genes (Shastry and Giblin, 1999). These variants lead to an early-onset AD by altering the processing of APP (Goate et al., 1991; Sherrington et al., 1995; Levy-Lahad et al., 1995). It has been shown that the Swedish double mutation in APP (K670N/M671L) strongly enhances APP cleavage by β-secretase 1 (BACE1), the major β-secretase involved in APP processing (Haass et al., 1995; Johnston et al., 1994). In rodent models, the Swedish mutation increases the production of Aβ and sAPPβ and decreases the levels of sAPPα (Hsiao et al., 1996; Tambini et al., 2019). In human CSF of Swedish mutation carriers, decreased levels of sAPPα and Aβ42 were observed (Lannfelt et al., 1995; Thordardottir et al., 2017). The London APP variant (V717I) has been shown to alter y-secretase cleavage of APP leading to increased levels of Aβ42 with little effect on Aβ40 levels (Goate et al., 1991; Suzuki et al., 1994). In human induced pluripotent stem cell (iPSC) derived neurons carrying the London mutation, an additional decrease in the levels of sAPPβ was observed (Muratore et al., 2014). A mutation in *PSEN1* resulting in the deletion of exon 9 (ΔE9) has been shown to increase the ratio of Aβ42/Aβ40 (Steiner et al., 1999; Crook et al., 1998; Prihar et al., 1999; Borchelt et al., 1996; Hiltunen et al., 2000). For the majority of AD cases, especially for the late-onset sporadic form of AD, no causal genetic mutations have been identified. The strongest genetic risk factor identified for sporadic AD is the ε4 allele of the *APOE* gene (*APOE4)* (Corder et al., *1993*; Strittmatter et al., *1993)*. Heterozygous carriers of *APOE4* have a 3-fold increased risk for AD compared to individuals with two copies of *APOE3*, while homozygous *APOE4* carriers have a 12-fold higher risk for AD (Corder et al., 1993). In contrast, the *APOE2* allele protects against AD (Corder et al., 1994). Genome-wide association studies (GWAS) and recent applications of next-generation sequencing (NGS) have enabled the identification of rare variants associated with AD, and over 80 AD risk loci with genome-wide significance have so far been identified (Khani et al., 2022; Bellenguez et al., 2022).

In 2012, a coding variant A673T (rs63750847) in *APP* was found to protect against AD and age-related cognitive decline in the Icelandic population (Jonsson et al., 2012). The APP A673T variation is adjacent to the APP Swedish mutation near the β-secretase cleavage site of APP. After α-secretase cleavage, APP A673T becomes part of sAPPα, while after cleavage through β- and γ-secretases, it becomes part of the Aβ peptide. The position of the APP A673T variation in relation to the secretase cleavage sites is shown in the Fig. S 1. In vitro studies suggest that the APP A673T variant protein is a less favorable substrate for β-secretase cleavage and that the generated Aβ peptides are less prone to aggregate and have a reduced binding affinity to synaptic receptors (Jonsson et al., 2012; Limegrover et al., 2021; Kimura et al., 2016; Maloney et al., 2014; Benilova et al., 2014). Overexpression of the APP A673T variant in human embryonic kidney (HEK) cells led to decreased levels of Aβ40, Aβ42, sAPPβ, and CTFβ by 25–40% as compared to the expression of wild-type (WT) APP (Jonsson et al., 2012; Maloney et al., 2014). In primary mouse cortical neurons, overexpression of the human APP A673T variant reduced levels of Aβ40 and Aβ42 as well as the ratio of sAPPβ relative to sAPPα as compared to WT APP-overexpressing neurons. Similar changes were observed in isogenic iPSC-derived human neurons carrying the APP A673T variant as compared to WT APP (Maloney et al., *2014)*. A biochemical in vitro approach showed that the introduction of the APP A673T variant reduces the catalytic turnover rate of APP by BACE1. While the observed decrease in sAPPβ and CTFβ levels, as well as enzyme activity assays, suggest reduced β-secretase cleavage of APP A673T, a study overexpressing CTFβ carrying the protective variation suggested reduced cleavage through γ-secretase (Kokawa et al., 2015). In this study, a reduction in Aβ and sAPPβ but not CTFβ levels was observed in T-REx CHO cells overexpressing APP A673T as compared to WT APP, and expression of CTFβ carrying A673T led to a decrease in Aβ production as compared to WT CTFβ (Kokawa et al., 2015).

In non-Nordic populations, the APP A673T variant is extremely rare or undetected (Liu et al., 2014; Wang et al., 2015). In the Finnish population, allelic frequencies for APP A673T between 0.10% and 0.52% have been found in different cohorts (Jonsson et al., 2012; Martiskainen

et al., 2017; Kero et al., 2013). A population-based study of 515 Finnish subjects found the APP A673T variant in one subject, who showed only little Aβ accumulation in neocortical tissue despite a very high age at death (104.8 years) (Kero et al., 2013). Our previous analyses in a population-based Metabolic Syndrome in Men (METSIM) cohort indicated that the carriers of the protective variant exhibited about 28% lower plasma levels of Aβ40 and Aβ42 (Martiskainen et al., 2017) as compared to control individuals.

Here, we have searched for the APP A673T variant in a large Finnish sample cohort consisting of AD patients and elderly control individuals, but also other neurodegenerative disorders to determine whether the variant shows a protective effect against AD and other neurological disorders. We further identified three carriers of the APP A673T variant among idiopathic normal pressure hydrocephalus (iNPH) patients. The typical treatment of iNPH patients comprises of CSF shunting, during which brain biopsies can be obtained from living patients (Torretta et al., 2021). Importantly, approximately 50% of iNPH patients show early (Aβ), or advanced AD-related brain pathologies (Aβ and tau) and thus, providing a unique opportunity to study the development and progression of AD-related pathology (Seppala et al., 2012). Furthermore, given the extremely low frequency of the *APP* A673T variant in most populations, the Finnish iNPH cohort made it possible to obtain and study brain and CSF samples of variant carriers for the first time. Here, we utilized these brain biopsies from iNPH patients together with CSF and plasma samples of the APP A673T carriers and matched controls to analyze them specifically for AD-related pathology. Additionally, an unbiased proteomics approach was used for analyzing these samples. The existing studies on APP A673T function have in common that they focused on the protective variant in a WT APP background in different cultured cells under basal conditions. We therefore investigated whether the introduction of the protective APP A673T variant alters the processing of APP in in vitro cell culture models of AD. Next to 2D cell cultures, we utilized a 3D human neural cell culture system that has been shown to exhibit key events in AD pathogenesis through the presence of both the Swedish and London mutations in APP (Kim et al., 2015). Collectively, we confirmed the protective effect of the APP A673T variant in the Finnish AD cohort and showed that the levels of both sAPPβ and Aβ42 were decreased in the CSF of APP A673T carriers. We further found that the protective APP A673T variant can shift APP processing towards the non-amyloidogenic pathway in vitro even in the presence of two pathogenic APP mutations. Finally, we identified differentially expressed proteins in the CSF and plasma of APP A673T carriers compared to controls. In general, a better understanding of the protective mechanisms of the APP A673T variant in carriers may provide insight into the disease pathogenesis and help to identify novel biomarkers as well as effective therapeutic strategies.

2. Methods

2.1. Study populations

AD patients and control individuals as well as patients with other neurological disorders (iNPH, vascular dementia (VaD), and mild cognitive impairment (MCI)) are part of the Finnish sample set of the European Alzheimer's Disease DNA BioBank (EADB). Demographics and GWAS-based genetic analysis of this sample set have been described in detail before (Bellenguez et al., 2022). Carriers of the APP A673T variant and matching controls for plasma, CSF, and biopsy analysis were selected from the Kuopio University Hospital (KUH) NPH Registry. The sample set and recruitment process have been previously described (Junkkari et al., 2019). RNA and protein expression data from Braak stage-classified post-mortem temporal cortical samples were obtained from a Finnish neuropathological cohort, which has been described in detail previously (Marttinen et al., 2019).

2.2. Plasma, CSF, and biopsy samples from APP A673T carriers and controls

Plasma and CSF sample collection from individuals of the KUH NPH Registry has been performed as described in detail before (Seppala et al., 2012). The right frontal cortical biopsy procedure has been described previously (Leinonen et al., 2010).

2.3. Sequencing

PCR-based *APOE* genotyping from blood samples was conducted as described earlier (Tsukamoto et al., 1993). For APP A673T genotyping, genomic DNA was extracted from blood samples and the region of interest was amplified using two specific primers (5′-CCACTTTAAGTCCCGAGTCA-3′ and 5′-TGGGAACACGGTAGAGAAGA-3′). Carrier status for the APP A673T variant was then confirmed by Sanger sequencing with a single primer (5′-GTAATCCTATAGGCAAGCATTG-3′).

2.4. Immunohistochemistry of cortical biopsies

The cortical biopsies were assessed for AD-related Aβ and tau pathology by immunostaining of paraffin sections with monoclonal antibodies directed to Aβ (6F/3D, M0872; Dako; dilution 1:100; pretreatment 80% formic acid 1 h), hyperphosphorylated tau (p-tau) (AT8, 3Br-3; Innogenetics; dilution 1:30) and sequestosome-1 (p62 lck ligand; BD Bioscience; dilution 1:1000; pretreatment: autoclaved at 120 °C in 0.01 mol/l citrate buffer, pH 6) as previously described (Leinonen et al., 2012; Rauramaa et al., 2013). Immunoreactivity of Aβ, p-tau, and p62 was then graded as present or absent in the sample by a neuropathologist. For immunofluorescence staining, antigen retrieval was performed by boiling the sections in 10 mM citrate buffer, pH 6.0 (for GFAP detection) or Tris-EDTA buffer, pH 9.0 (for IBA1 detection) for 10 min, and autofluorescence was reduced by incubation with 1× TrueBlack lipofuscin autofluorescence quencher (23007, Biotium) in 70% ethanol for 30 s. Samples were blocked in 3% bovine serum albumin (BSA) and incubated with the primary antibody GFAP (rabbit polyclonal, Z0334; Dako; dilution 1:1000) or IBA1 (rabbit polyclonal, 019–19741; Wako; dilution 1:1500) at 4 °C overnight. The samples were then incubated with the secondary antibody for 1 h at room temperature (Anti-rabbit-Alexa-488 (from goat), A11008; Invitrogen, dilution 1:500 or Anti-rabbit Alexa-568 (from goat), A11036, Invitrogen, dilution 1:500) and DNA (nuclei) was stained with 1 μg/ml DAPI (D1306, Fisher Scientific) for 5 min. Images were taken with a Zeiss Axio Observer inverted microscope equipped with an LSM 800 confocal module (Carl Zeiss Microimaging GmbH) using a 20 × (NA 0.5) objective.

2.5. CSF biomarker analysis

CSF levels of Aβ42, t-tau, and p-tau 181 were measured as described previously (Seppala et al., 2012). The interassay coefficients of variation (CV%) were 5.7% for Aβ42, 4.7% for tau, and 6% for p-tau 181. The intra-assay coefficients of variation were 2% for Aβ42, 4.2% for t-tau, and 4.8% for p-tau 181. Aβ40 levels in CSF were determined using Human/Rat βAmyloid(40)ELISA Kit II (294–64701; Wako). CSF levels of total soluble APP (sAPPtot = sAPPα + sAPPβ), sAPPα, and sAPPβ were measured using highly sensitive ELISA kits (27734, 27732, and 27731, Immuno-Biological Laboratories) according to the manufacturer's instructions. All samples were measured in duplicates and diluted before the measurement (Aβ40 1:30; sAPPtot 1:150; sAPPα 1:100; and sAPPβ 1:25). The intra-assay coefficients of variation were 2.8% for Aβ40, 2.7% for sAPPtot, 5.2% for sAPPα and 1.6% for sAPPβ.

2.6. Proteomics sample preparation

For proteomics analysis, we have used six plasma and six CSF

samples from each of the three heterozygous carriers of APP A673T mutation (two male and one female) and three age- and sex-matched control individuals. We have applied a TMT®-based Calibrator approach for multiplexed proteomics (Dayon et al., 2010) using brain lysate as Calibrator tissue. The total protein concentration of plasma and CSF was determined by a modified Bradford protein assay and each sample was visualized by Coomassie-stained (Imperial Stain, Pierce) SDS-PAGE 4–20% gradient gels (Criterion, Biorad; data not shown).

Three brain cortex tissues (Braak Stage 0) were lysed in 8 M urea, 75 mM NaCl, and 80 mM Tris; pH 8.2 containing phosphatase and protease inhibitors. Tissue debris was removed by centrifugation at 12000*g*, 4 °C for 2x10min. The protein concentration was determined by the Bradford assay and the protein content was visualized by Coomassie-stained (Imperial Stain, Pierce) SDS-PAGE 4–20% gradient gels (Criterion, Biorad; data not shown). 1.98 mg of each brain lysate was used to generate a pooled brain lysate that was used as a brain Calibrant sample.

A tandem IgY14/Super depletion method was used to deplete high and medium abundant proteins from 6 plasma samples. Plasma volumes corresponding to ~12.5 mg of protein were immuno-affinity-depleted of the 14 most abundant plasma proteins followed by the next ~50 moderately abundant proteins (Keshishian et al., 2017) using mouse Seppro® IgY14 (LC10) and Seppro® Supermix (LC5) columns (Sigma-Aldrich, St. Louis, MO, USA). In an FPLC-assisted manner (Knauer) plasma samples were loaded on the IgY14 column and the flow-through was directed onto the Supermix column. Dilution, stripping, and neutralization buffers were used, and the manufacturer's instructions were followed (Sigma-Aldrich). Flow-through that included protein based on UV absorbance was collected and concentrated by spin filters (Amicon 3 kDa MWCO; Millipore) to a volume of ~250–360 µl. The protein concentrations of the samples post-depletion were determined using a modified Bradford Assay and the protein content was visualized by Coomassie-stained (Imperial Stain, Pierce) SDS-PAGE 4–20% gradient gels (Criterion, Biorad).

Protein Digestion and TMT® Labeling:

Calibrant brain sample: The pooled brain lysate was reduced (at 56 °C for 25 min with 5 mM dithiothreitol (DTT)), alkylated (at room temperature for 30 min in the dark with 14 mM iodoacetamide (IAA)), quenched with DTT 5 mM for another 15 min and digested overnight with trypsin (Promega, sequencing grade) after dilution to 1.6 M urea at 37 °C to generate peptides. The digests were combined to produce a pool and desalted (SepPak tC18 cartridges). The pooled brain digest was split into 4 aliquots in a protein mass ratio of 1:4:6:10 and dried in a speedvac without heating. The four aliquots were solved in 50 mM KH_2PO_4 at pH 4.5 and labeled with TMT® 10plex reagents 129C, 130N, 130C, and 131, respectively. Labeled samples were treated with hydroxylamine and combined. The mixed Calibrant brain sample was stored at −80 °C until used to be combined with the labeled and mixed plasma or CSF samples (see below).

Depleted plasma samples: 40 µg per each of the six depleted plasma samples was used per reaction. Depleted plasma samples were brought to equal volumes using Seppro dilution buffer (Sigma-Aldrich) and used for digestion and TMT® labeling. All samples were reduced using 5 mM DTT for 25 min at 56 °C, alkylated using 14 mM IAA for 30 min at room temperature, quenched with DTT 5 mM for another 15 min, and digested with trypsin to generate peptides, desalted (SepPak tC18 cartridges) and dried in a speedvac without heating.

Dry peptides were dissolved in 50 mM KH_2PO_4, pH 4.5. Peptides were mixed with one TMT® 10plex reagent (126, 127N, 127C, 128N, 128C, and 129N for samples APP A673T 1, 2, 3 and control 1, 2, and 3, respectively). Labeled samples were treated with hydroxylamine and the appropriately labeled digests were pooled to generate the TMT® 10plex samples (per TMT® 10plex: 6 plasma samples (6 × 40 µg) + brain calibrator mix (~420 µg) in a protein mass ratio of 1:1.75). 50 µg of the mixed 10plex was purified by solid-phase extractions for LC-MS analysis to be used for assessment of labeling efficiency and reporter ion distributions. The remaining 10plex mixtures were purified using SepPak tC18-cartridges and a portion of ~300 µg was used for basic reversed-phase fractionation. Fractionation of the mixed 10plex was performed using HPLC-assisted basic reversed-phase (bRP) chromatography (EC 250/4.6 Nucleodur C18 Gravity (Macherey-Nagel) on a Waters Alliance 2695 HPLC system. In total, 54 tubes were collected at regular time points along the main elution profile for the separation. These were combined to generate 30 fractions of the plasma TMT® 10plex sample.

CSF samples: 300 µg of protein from each of the 6 CSF samples was used. CSF samples were brought to equal volumes with water and diluted with a quarter of the volume of 8 M urea, 120 mM NaCl, 250 mM Tris, pH 8.2 containing protease inhibitors (Complete Mini, Roche) and phosphatase inhibitors (PhosStop, Roche). All samples were reduced and alkylated as described above, diluted with 25 mM Tris, 1.6 M urea, pH 8.2 and digested with trypsin to generate peptides, desalted (SepPak tC18 cartridges), and dried in a speedvac without heating.

Dry peptides were dissolved in 50 mM KH_2PO_4, pH 4.5. Peptides were mixed with their respective TMT® 10plex reagent (126, 127N, 127C, 128N, 128C, and 129N for samples APP A673T 1, 2, 3 and control 1, 2, and 3, respectively). Individual TMT® reactions were terminated with hydroxylamine and the appropriate labeled digests were pooled to generate the TMT® 10plex samples (6 CSF samples (~1800 µg) + brain calibrator mixture (~3150 µg) in a protein mass ratio of 1:1.75). 50 µg of the mixed 10plex was purified by solid-phase extractions for LC-MS analysis to be used for assessment of labeling efficiency and reporter ion distributions. The remaining 10plex mixture was purified using SepPak tC18-cartridges and dried in portions of 4700 µg (for phosphopeptide enrichment) and 2 × 100 µg (for basic reversed-phase of the non-enriched samples and backup).

The CSF TMT® 10plex sample was enriched for phosphopeptides using the High Select™ Fe-NTA Phosphopeptide Enrichment Kit (Thermo Scientific) according to the manufacturer's instructions in a batch process split over two columns yielding one phosphopeptide fraction.

Basic reversed-phase fractionation of the CSF 10plex sample was conducted for A) 100 µg of non-enriched sample and B) enriched phosphopeptides. Here, the Pierce™ High pH Reversed-Phase Peptide Fractionation Kit (Thermo Scientific) was used according to the manufacturer's instructions to produce 8 fractions. For the phosphopeptides, fractions 1 to 6 were used for MS-analysis. For the non-enriched peptides, fractions 1 and 2 and fractions 7 and 8 were combined to finally produce 6 fractions for MS-analysis.

2.7. Liquid chromatography mass spectrometry analysis

2.7.1. Data acquisition

All samples were analyzed on an Easy-nLC 1000 nano liquid chromatography system coupled to an Orbitrap Fusion Tribrid mass spectrometer (both Thermo Scientific). Peptides were resuspended in 2% acetonitrile (ACN) 0.1% formic acid (FA) and trapped on a nanoViper C18 Acclaim PepMap 100 trap column (75 µm i.d. x 20 mm, Thermo Scientific), then resolved over a 50 cm EasySpray RSLC analytical column (75 µm i.d. x 500 mm, Thermo Scientific). Mobile phases had the following composition: A (aqueous phase): 0.1% FA in H2O; B (organic phase): 0.1% FA in ACN. All solvents used were HPLC grade (Biosolve).

For plasma samples, the employed linear gradient ranged from 6% B to 35% B over a total duration of 104 min, followed by a 16 min washout which included an increase to 90% B. For CSF samples, the linear gradient ranged from 10% to 30% B over 160 min, followed by a 20 min washout phase. In all cases, a pre-equilibration step to gradient starting conditions was included before the loading of the sample.

All data was acquired in data dependent mode, with largely similar settings for plasma and CSF. MS1 scans were acquired at 120 K resolution in 3 s intervals with automatic gain control (AGC) set to 5e5 (plasma) or 2e5 (CSF). Precursors were picked from an inclusion list of previously identified APP-derived peptides and phosphopeptides, when no pre-specified precursors were observed, the method defaulted to

fragmenting precursors in order of decreasing intensity. Precursors were isolated in 1.2 *m/z* isolation windows and fragmented by higher energy collision induced dissociation (HCD) at a setting of 38. Resulting fragments were acquired at a resolution of 30 K (plasma) or 60 K (CSF) with AGC set to 1e5 in both cases. The intensity threshold for an MS2 scan was set to 25,000. After being fragmented once a precursor was excluded from repeated fragmentation for 20 s (plasma) or 30 s (CSF), respectively.

2.7.2. Computational mass spectrometry

All mass spectrometry data files were processed in Proteome Discoverer (PD) v2.1 (Thermo Scientific). Spectra were searched against a human UniProtKB reviewed database (version from April 2019) appended with mutant APP variants and a database of common laboratory contaminants using the SEQUEST HT search engine. The enzyme specificity was set to trypsin, with the search allowing for up to 2 missed cleavages. The precursor mass tolerance was set to 10 ppm, while the fragment tolerance was set to 0.02 Da. TMT modification of N-termini and lysines, and carbamidomethylation of cysteines were set as static modifications, while methionine oxidation was set as a variable modification. Phosphorylation of serine, threonine, and tyrosine was considered as a variable modification and localization probabilities of phosphorylation sites were determined using ptmRS (Taus et al., 2011). After the first round of search with full tryptic specificity, all spectra with no associated high confidence sequence assignments were searched again allowing one non-tryptic peptide terminus. All TMT-reporter intensity values were exported to tab-delimited text files for later processing and filtering. Peptide spectrum match (PSM) results were filtered at 1% (High confidence) false discovery rate (FDR) using Percolator (Käll et al., 2007) and exported for biostatistical processing.

2.8. Bioinformatics analysis of mass spectrometry data

For CSF and Plasma samples: PSMs with isolation interference values >50% were removed. TMT® reporter intensities were then corrected for isotopic impurities and median scaling applied to the data matrix. Reporter ion intensities were then re-calculated relative to the median across reference channels and $\log_2$-transformed. Peptide expression values were computed as the median across all related PSMs. Peptides with >35% missing values in at least one experimental group were removed. Among the remaining peptides, missing values were imputed using an iterative PCA method (Josse and Husson, 2016). Protein expression was calculated as the trimmed mean (trim factor = 0.2) across all unmodified peptides distinct to the protein group. To identify peptides, phosphopeptides, or proteins significantly changing in abundance between clinical groups, we applied moderated t-statistics (Ritchie et al., 2015), which is very suited for small data sets. A linear model with one clinical factor (mutation status) was applied: *gRatio*~-*Class*. Factor *Class* has two levels: (APP and Control; reference level = Control). The log fold change threshold was set to exceed the two times features average standard deviation.

Significance of enrichment analyses were performed to highlight biological functions overrepresented among differentially abundant features. Two-sided *p*-values were generated and the Benjamini-Hochberg method (Benjamini and Hochberg, 1995) was used for multiple test correction.

2.9. Neprilysin assay from human plasma

Plasma samples for measurement of neprilysin levels were part of the population-based Metabolic Syndrome in Men (METSIM) study. The study design as well as APP A673T carrier information and the selection of the control group have been described previously (Martiskainen et al., 2017; Stancáková et al., 2009). Neprilysin levels from plasma samples were measured using Human Neprilysin DuoSet ELISA Kit (DY1182, R&D Systems) together with DuoSet ELISA Ancillary Reagent Kit (DY008, R&D Systems) according to the manufacturer's instructions. Neprilysin concentration was below the limit of quantitation (<29 pg/ml) in 18% of the samples (48/261).

2.10. Plasmid DNA and lentiviral vectors

Lentiviral polycistronic vectors (CSCW-IRES-GFP, CSCW-APPSL-IRES-GFP (APP-SL), CSCW-IRES-mCherry, and CSCW-IRES-PSEN1 (ΔE9)-mCherry) were the same as used in Choi et al.,2014 (Choi et al., 2014). CSCW-APPSL(A673T)-IRES-GFP (APP-SL-A673T) was constructed by site-directed mutagenesis (Quik-Change Lightning Multi Site-Directed Mutagenesis Kit, Agilent, 210,515). Briefly, the CSCW-APPSL-IRES-GFP vector DNA was mutagenized with a single primer (5′-CTCTGAAGTGAATCTGGATACAGAATTCCGACATGACT-3′). The remaining original plasmid DNA was subjected to *Dpn*I restriction digest, and the mutagenized plasmid DNA was then transformed into XL10-Gold® ultracompetent cells (Agilent). The integrity of the construct and introduction of the A673T variant were confirmed by Sanger sequencing using the following primers: 5′-AGGATGAAGTTGATGAGCTG-3′, 5′-TTCTGCATCTGCTCAAAGAA-3′, 5′-TTCACTAATCATGTTGGCCA-3′, 5′-TTCTGTGTCAAAGTTGTTCC-3′ and 5′-GAGAAGGGCATCACTTACAA-3′. The packaging of the constructs into third-generation self-inactivating lentiviral particles was performed by the National Virus Vector Laboratory (University of Eastern Finland, Kuopio, Finland).

2.11. HEK cell culture and transfection

HEK293-AP-APP cells expressing alkaline phosphatase (AP)-conjugated APP695 (Lichtenthaler et al., 2003) were cultured in Dulbecco's Modified Eagle Medium (DMEM) with 4.5 g/l glucose (BE12-614F, Lonza), 10% (*v*/v) fetal serum albumin (FBS, 10270–106, Gibco), 2 mM L-glutamine (17-605E, Lonza), 50 μg/ml hygromycin B and 0.3 μg/ml puromycin. For transfection, 4×10^5 cells/well were plated on poly-D-lysine (P6407, Sigma–Aldrich) coated 6-well plates (140675, Nunc A/S) and incubated with 2.5 μg/well DNA and Lipofectamine™ 2000 Transfection Reagent (11668019, Invitrogen) according to the manufacturer's instructions. After 24 h, the cells were washed twice with DPBS (17-512F, Lonza) and fresh culture medium was added. The cells and the conditioned medium were collected after another 24 h.

2.12. ReN cell culture, transduction, and treatment

ReNcell® VM human neural progenitors (ReN cells) were maintained in DMEM/F12 (Life Technologies) medium supplemented with 2 mg/ml heparin (07980, StemCell Technologies), 2% (*v*/v) B27 neural supplement (17504044, Fisher Scientific), 1% (v/v) penicillin/ streptomycin/ amphotericin-b solution (17-745E, Lonza), 20 mg/ml hEGF (E9644, Sigma-Aldrich) and 20 mg/ml bFGF (03–0002, Stemgent). Culturing and transduction of the cells were conducted as described in detail by Kim et al. (Kim et al., 2015). In brief, for transduction, ReN cells were dislodged from a confluent T25 flask (C6481, Greiner) and distributed into six Matrigel (356230, Corning) coated wells of a 6-well plate. The cells were left to settle overnight and when a confluence of ~80% was reached, 6×10^6 transducing units (TU) of viral particles were added per well to achieve a multiplicity of infection (MOI) of approximately 1. The cells were cultured overnight, washed twice, and cultured for 2–3 more days until GFP or mCherry signal could be observed by fluorescence microscopy. For 2-dimensional cell culture experiments, the transduced cells were split in a ratio of 1:4 to new Matrigel-coated 6-well plates. When the cells reached a confluency of ~80%, a 15-day differentiation process into neurons was started by depriving growth factors hEGF and bFGF from the culture medium (differentiation medium) and exchanging the medium every 2–3 days. On day 14 of differentiation, γ-secretase inhibitor treatment was started by adding 1 μM DAPT (D5942, Sigma) in fresh differentiation medium 24 h prior to sample

collection.

2.13. 3D ReN cell culture

ReN cells were transduced as described above and thick-layer 3D cultures were established as described in detail before (Kim et al., 2015). In brief, transduced ReN cells were sorted through fluorescence-activated cell sorting (FACS) using a FACS Aria III sorter (Becton Dickinson) to select cells with the highest levels of GFP only or GFP and mCherry expression. To expand the cells, the sorted cells were passaged three times and stored in liquid nitrogen until plating. To prepare the 3D cultures, 2×10^7 cells/ml were mixed 1:1 (v/v) with ice-cold Matrigel, and 300 µl of the suspension was transferred to each tissue culture insert (10421761, Falcon) of 24-well plates (142475, Nunc A/S). On the next day, 500 µl differentiation medium was added to the insert and surrounding well respectively. Half of the medium was exchanged every 3 days for 14 weeks. The culture quality was monitored through regular LDH release assays and parallel plating of thin-layer 3D cultures and fluorescence microscopy as described in detail by Kim et al. (Kim et al., 2015).

2.14. Protein extraction and Western blot analysis

To prepare protein lysates for Western blot analysis from 2D cell cultures, the cultured cells were washed twice with PBS and lysed in T-PER Tissue Protein Extraction Reagent (78510, Thermo Fisher Scientific) supplemented with protease and phosphatase inhibitor (87785 and 78420, Thermo Fisher Scientific). After 30-min incubation of the suspension on ice, cell debris was removed by centrifuging for 10 min at 10,000 ×g. Protein extraction from 3D cell cultures was conducted as described in detail before (Kim et al., 2015). Briefly, proteins were extracted from the Matrigel pellet in three extraction steps: once with 2× TBS extraction buffer and twice with 2× RIPA extraction buffer each followed by sonication, homogenization with a rotor-driven homogenizer, and centrifugation at 10,000 ×*g* for 5 min at 4 °C. The protein concentration of the lysates was measured with the Pierce BCA Protein Assay Kit (23227, Thermo Fisher Scientific), and 20–35 µg total protein per sample was incubated at 55 °C for 10 min with NuPAGE LDS Sample Buffer (NP0007, Invitrogen). Proteins were separated on NuPAGE 4–12% BisTris Midi Protein Gels (WG1202BOX, Invitrogen) and SeeBlue Plus2 Pre-stained Protein Standard (LC5925, Invitrogen, Carlsbad, CA, USA) was used for size determination. The proteins were then transferred onto PVDF membranes (IB24001, Thermo Fisher Scientific) with an iBlot 2 Gel Transfer Device (IB21001, Thermo Fisher Scientific) and the blots were probed at 4 °C overnight with the following antibodies: 22C11 (1:1000, MAB348, Merck, anti-APP N-terminal, detection of sAPPtot), 6E10 (1:1000 SIG-39320, Covance, for detection of sAPPα), sAPP beta wild type (JP18957, IBL international), β-actin (1:1000, ab8226, Abcam), GAPDH (1:5000, ab8245, Abcam), Map2 (1:1000, M9942, Sigma), p-GSK3β ser9 (1:1000 9336, Cell Signaling), GSK3β (1:1000, 9315, Cell Signaling), and C66 (1:1000, anti-APP N-terminus, CTF and APP full-length detection), which was a kind gift from Dr. Dora M. Kovacs (Bhattacharyya et al., 2013). After incubation with mouse or rabbit immunoglobulin G (IgG) horseradish peroxidase-linked secondary antibody (1:5000, GENA931 or NA934, GE Healthcare) for 1 h, proteins were detected with ECL Select or Prime Western Blotting Detection Reagent (12644055 or 12316992, GE Healthcare) and a ChemiDoc Imaging System (Bio-Rad Laboratories). Image Lab Software 6.0.1 (Bio-Rad Laboratories) was used to quantify protein levels.

2.15. Soluble APP measurements from conditioned medium

For the detection of sAPP and Aβ, conditioned medium was collected from the 2D and 3D ReN cell cultures prior to cell collection and centrifuged for 10 min at 10,000 ×g. sAPPα, sAPPβ, and sAPPtot levels were measured using highly sensitive ELISA kits (27734, 27733, and 27731, Immuno-Biological Laboratories) as instructed by the manufacturer. The chosen sAPPβ ELISA kit is specialized on the detection of sAPPβ harboring the Swedish variant (sAPPβ-sw). Aβ40 and Aβ42 levels were measured using Human/Rat βAmyloid(40)ELISA Kit II and Human/Rat β Amyloid (Torretta et al., 2021) ELISA Kit (294–64701 and 292–64501; Wako).

2.16. Statistical analyses

Apart from the mass spectrometry data analysis, all statistical analyses were conducted using Prism 9 (GraphPad Software). For odds ratios, Gart adjusted logit confidence interval was calculated to correct for zero values. *P*-values for the odds ratios were obtained from two-sided Fisher's Exact Test. For comparisons between groups, the Shapiro-Wilk normality test was used to analyze data distribution. Independent samples *t*-test or independent samples Mann–Whitney *U* test was used to test for statistically significant differences between two groups depending on the distribution of the data. One-way ANOVA and Tukey's multiple comparisons test or Kruskal-Wallis test and Dunn's multiple comparisons test were used to compare three or more groups. For correlation analyses, Spearman's rho and Pearson correlation test were used. Statistical significance was set at $p < 0.05$ for all tests.

3. Results

3.1. The APP A673T variant protects against AD in a Finnish sample set and decreases the levels of sAPPβ and Aβ42 in the CSF samples

In the Finnish EADB (*European Alzheimer's Disease BioBank*) sample set (Bellenguez et al., 2022), comprising of 1070 AD cases (mean onset age 70.9 ± 8.8) and 2122 controls (mean age at the time of examination 71.8 ± 7.1), we found 13 heterozygous *APP* A673T carriers in the control group and none in the AD group (Table 1). This results in an allelic frequency of 0.31% for the *APP* A673T variant in the control sample set of elderly Finnish individuals. Thus, the minor allele (C > T) resulting in the A673T substitution in APP was found to be significantly more common in the elderly control group than in the AD group with an odds ratio (OR) = 0.07, confirming the protective effect against AD (Table 1). Subsequently, we examined the frequency of the *APP* A673T in individuals with other neurodegenerative disorders and iNPH. While we did not find the *APP* A673T variant in patients with VaD or AD-iNPH, the frequency of the *APP* A673T variant was similar in iNPH, MCI and AD-VaD individuals as compared to controls. In these groups, the OR did not reach statistical significance, most likely due to the small sample size.

As three carriers of the *APP* A673T variant were detected in a Finnish cohort of patients with possible iNPH, three iNPH patients not carrying the *APP* A673T variant from the same cohort were individually matched according to age at the time of shunt operation (±3 years), sex, *APOE* genotype as well as neuropathological findings to serve as controls for the following analyses (Table 2). The controls were chosen from the iNPH cohort because it has been previously shown, that levels of AD-related peptides, such as sAPP and Aβ differ significantly in the CSF of iNPH patients as compared to healthy controls (Moriya et al., 2015). Importantly, since the biopsy samples obtained from the frontal cortex of three *APP* A673T carriers did not show Aβ, phospho-tau (p-tau), or p62 pathology according to preexisting IHC analysis data, iNPH patients not showing the Aβ, p-tau, or p62 pathologies in the biopsy samples were selected as controls. The presence of the *APP* A673T variant was confirmed using Sanger sequencing for the three studied individuals. To further elucidate the status of the *APP* A673T and control tissue samples, we performed IHC staining on frontal cortical brain biopsy samples. IHC staining of the astrocytic marker GFAP and the microglial marker IBA1 did not show major differences in GFAP- or IBA1-positive cell morphology or distribution between biopsies from *APP* A673T carriers and controls (Fig. S 2).

Table 1
Genotype frequencies of the *APP* A673T variant in different disease and control cohorts.

APP A673T C>T[a]		Cohort							
		Control	AD	AD-iNPH	iNPH[b]	AD-VaD[b]	MCI	VaD	Total
CC	Count	2109	1070	14	482	16	184	67	3942
	%	99.4	100.0	100.0	99.6	94.1	98.9	100.0	99.5
TC	Count	13	0	0	2	1	2	0	18
	%	0.6	0.0	0.0	0.4	5.9	1.1	0.0	0.5
Total	Count	2122	1070	14	484	17	186	67	3960
OR		–	0.07	5.49	0.67	9.86	1.76	1.17	
95% CI		–	0.004–1.2	0.3–94.7	0.2–3.0	0.9–55.6	0.4–6.6	0.07–19.7	
p-value		–	0.007	n.s.	n.s.	n.s.	n.s.	n.s.	

Abbreviations: AD = Alzheimer's disease; AD-iNPH = AD and idiopathic normal pressure hydrocephalus; iNPH = idiopathic normal pressure hydrocephalus; AD-VaD = AD and vascular dementia (mixed form of dementia); MCI = mild cognitive impairment; VaD = vascular dementia; OR = odds ratio; compared to Control group.
[a] dbSNP ID: rs63750847.
[b] Biopsies from frontal cortex of *APP* A673T carriers did not show Aβ or tau pathology.

Table 2
Demographic and clinical characteristics of the studied *APP* A673T and control individuals.

Individual	*APP* A673T C>T[a]	Age	Sex	*APOE* genotype
***APP* A673T 1**	TC	76	Male	33
Control 1	CC	74	Male	33
***APP* A673T 2**	TC	71	Female	33
Control 2	CC	74	Female	33
***APP* A673T 3**	TC	79	Male	34
Control 3	CC	79	Male	34

[a] *APP* A673T carrier status was confirmed by Sanger sequencing.

So far, the effect of the protective variant on APP-derived metabolites has only been investigated in plasma samples of *APP* A673T variant carriers (Martiskainen et al., 2017). Since CSF is of particular importance for studying neurological disorders, we measured the levels of AD-associated biomarkers in the CSF from *APP* A673T carriers and respective controls (Fig. 1). In the CSF samples from *APP* A673T carriers, sAPPβ levels were significantly decreased on average 9% as compared to the age-, sex-, *APOE,* and brain pathology-matched controls. Similarly, Aβ42 levels were 26% lower in the CSF from *APP* A673T variant carriers as compared to controls. Also, the levels of Aβ40 showed a trend towards a reduction in APP A673T variant carriers, but this result did not reach statistical significance ($p = 0.086$). No statistically significant differences were detected in the levels of sAPPtot, sAPPα, p-tau, or total-tau (t-tau). Collectively, these results indicate that the *APP* A673T variant exerts protection against AD and AD-associated pathologies in the brain tissue, coinciding with the decreased levels of sAPPβ and Aβ42 in the CSF of individuals carrying the protective *APP* variant.

3.2. Unbiased mass spectrometry-based proteomics analysis of plasma and CSF samples obtained from APP A673T carriers detects differentially regulated targets involved in protein phosphorylation, inflammation, and mitochondrial function

To identify protein alterations in the CSF and plasma between the *APP* A673T carriers and controls in an untargeted fashion, the samples were analyzed using a mass spectrometry (MS)-based proteomics approach. Additionally, an MS-based phosphoproteomics assay was used to determine differences in phosphorylation levels of proteins in the CSF of *APP* A673T carriers as compared to controls. Despite the small sample size, sets of differentially regulated proteins, peptides, and phosphopeptides were found between the samples (Fig. 2a). In the CSF samples, more proteins were down-regulated than up-regulated in *APP* A673T carriers as compared to controls (7 proteins upregulated and 19 proteins downregulated with an FC threshold of 1.6 and $p < 0.01$) from a total of 3816 quantified proteins. In the plasma of *APP* A673T carriers, a similar number of proteins were down- and up-regulated as compared to controls (24 proteins upregulated and 26 proteins downregulated with an FC threshold of 1.5 and $p < 0.01$) from a total of 7985 quantified proteins.

Next, we looked at the biological processes found to be significantly over-represented by the differentially represented peptides in the CSF and plasma from *APP* A673T carriers compared to controls (Fig. 2b).

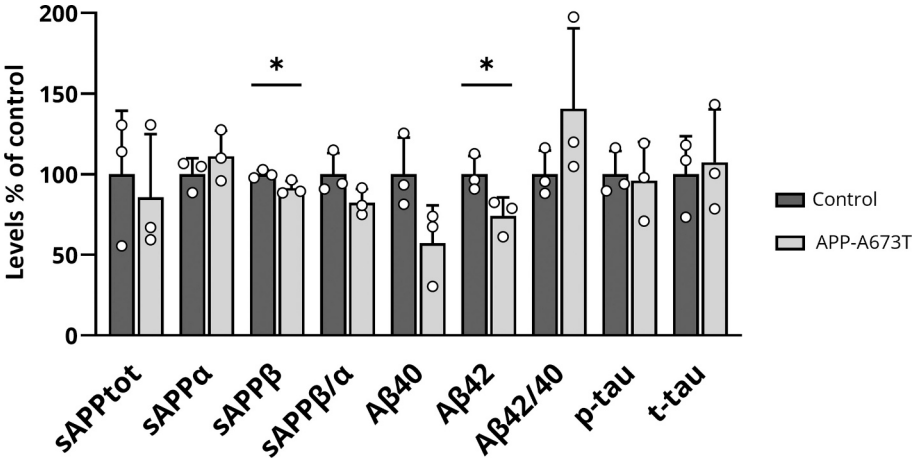

Fig. 1. sAPPβ and Aβ42 levels are significantly reduced in CSF samples of APP A673T variant carriers as compared to controls. Peptide levels were measured with ELISA from CSF samples. Levels of sAPPα and sAPPβ were normalized to sAPPtot (total levels of soluble APP α + β). Data are shown as mean + SD of n = 3 individuals. Independent samples t-test; *$p < 0.05$.

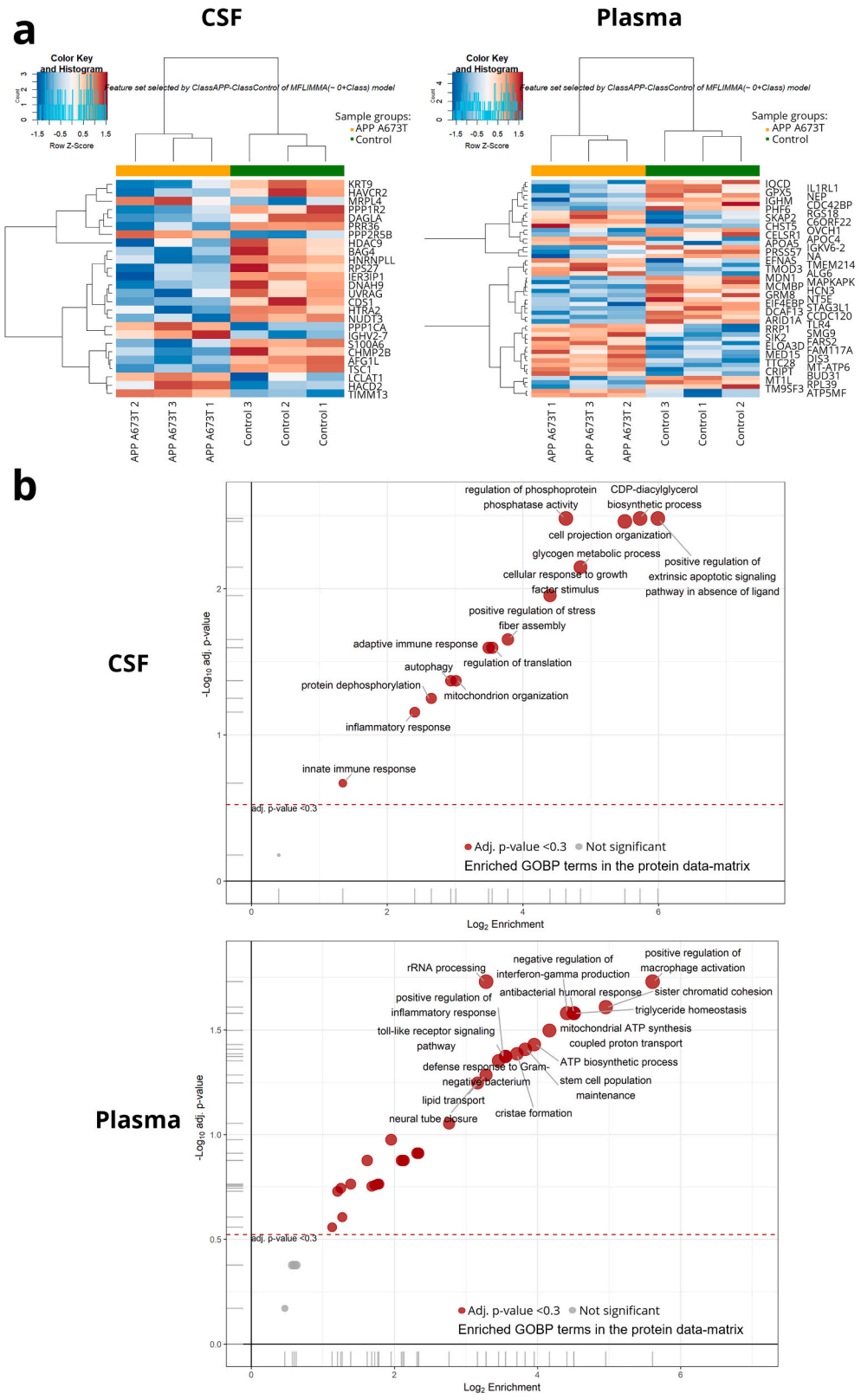

Fig. 2. Differentially expressed proteins in CSF and plasma from APP A673T carriers as compared to control individuals. a) Heatmap of regulated features, protein levels, three brain tissue (Braak Stage 0) lysates were used as a calibrator. Left panel: CSF, features displayed passing FC threshold 1.6 (logFC ~2·mean·(SD (proteins))) with $p < 0.01$. Right panel: plasma, features displayed passing FC threshold of 1.5 with $p < 0.01$. b) Top 20 most significantly (based on *p*-value) enriched GO biological processes in the CSF and plasma. Volcano plots showing $\log_2$ enrichment against significance of enrichment, highlighting the biological processes found to be significantly overrepresented by the differentially expressed peptides in the data set. No underrepresented terms were found. Filled red circles highlight significant hits (FDR < 0.3, red dashed line on the plot) with the size related to the corresponding rank value. (For interpretation of the references to colour in this figure legend, the reader is referred to the web version of this article.)

Overlapping processes found both in CSF and plasma were related to the regulation of protein phosphorylation, inflammatory response, and processes important for mitochondrial function.

Among the 20 most significantly differentially expressed proteins in the CSF from *APP* A673T carriers (Table 3), there were several proteins with a known relationship to AD pathology. The strongest decrease was observed for S100A6, which was decreased by 2.7-fold in the *APP* A673T carrier CSF as compared to control CSF. Levels of HAVCR2 and HTRA2 were decreased by 2- and 2.5-fold, respectively, in the CSF from *APP* A673T carriers. Two protein phosphatase subunits showed an increase in the CSF from *APP* A673T carriers as compared to controls: PPP1CA, a catalytic subunit of protein phosphatase 1 (PP1) complex, and PPP2R5B,

Table 3
Top 20 regulated features in the CSF and plasma of *APP A673T* carriers as compared to controls.

CSF						Plasma		
Proteins			Phosphopeptides			Proteins		
Gene name	log_2FC	p-value	Gene name	log_2FC	p-value	Gene name	log_2FC	p-value
S100A6	−1.456	4.72E-04	***CALHM6***	−3.247	8.31E-04	***NEP***	−1.823	3.17E-04
PRR36	−1.436	3.41E-04	***HERC1***	−2.116	4.07E-04	***BUD31***	−1.508	5.13E-04
HAVCR2	−1.342	1.91E-03	***SRRM2***	−1.477	5.81E-04	***DCAF13***	−1.338	3.96E-04
BAG4	−1.334	2.07E-03	***PCLO***	−1.476	8.93E-04	***STAG3L1***	−1.265	6.30E-04
RPS27	−1.29	3.49E-03	***EIF3CL***	−1.072	1.32E-02	***PHF6***	−1.136	9.88E-04
DNAH9	−1.217	1.63E-03	***FXYD1***	−0.936	9.98E-03	***ARID1A***	−1.116	1.77E-03
IER3IP1	−1.055	1.74E-03	***C2CD2L***	0.977	1.20E-02	***HCN3***	−0.966	2.63E-03
CDS1	−1.049	1.09E-03	***CACNB4***	1.382	1.51E-02	***OVCH1***	−0.809	3.52E-03
KRT9	−1.009	2.57E-03	***WDR20***	1.425	7.56E-04	***MT1L***	−0.806	2.05E-03
AFG1L	−1.008	5.52E-04	***MAP2***	1.514	6.94E-04	***MDN1***	−0.752	2.36E-03
HTRA2	−0.985	4.97E-03	***ADD3***	1.522	1.04E-03	***CCDC120***	−0.749	1.55E-03
UVRAG	−0.974	5.97E-03	***STX1A***	1.601	5.48E-04	***RPAP1***	−0.58	2.67E-03
TSC1	−0.94	5.84E-04	***PRKG2|C2CD4C***	1.623	7.46E-04	***RPS27L***	−0.538	3.78E-03
DAGLA	−0.883	5.92E-03	***GAS2L1***	1.63	8.35E-04	***GRAMD1B***	0.551	3.12E-03
HNRNPLL	−0.86	2.32E-03	***ANK2***	1.793	1.41E-04	***DIS3***	0.747	2.22E-03
NUDT3	−0.706	4.34E-03	***ARHGAP21***	1.837	3.29E-04	***CRIPT***	0.778	3.63E-03
PPP2R5B	0.746	3.23E-03	***ADTRP***	1.99	1.17E-03	***MED15***	0.885	3.77E-03
IGHV2-70D	0.895	3.07E-03	***MARCKS***	2.345	5.21E-04	***ATP5MF***	0.965	1.80E-03
TIMM13	0.923	6.61E-04	***MAP2***	3.064	1.76E-05	***ELOA3D***	1.087	2.39E-03
PPP1CA	1.879	2.28E-04	***GBF1***	3.616	8.90E-06	***TTC28***	1.357	7.45E-05

Relative expression is shown as log_2FC (log_2 fold change) in *APP* A673T carriers with respect to controls. P-value of moderated t-statistics for given protein contrast log_2FC. Top 20 regulated features (based on p-value) are sorted from lowest to highest relative expression.

a regulatory subunit of protein phosphatase 2A (PP2A), were increased by 3.6- and 1.7-fold, respectively, in the CSF from *APP* A673T carriers with respect to controls. Phosphopeptide analysis of CSF samples revealed two phosphorylated microtubule-associated protein 2 (MAP2) peptides among the 20 most significantly differentially expressed phosphopeptides (Fig. S 3). Levels of the MAP2 phosphopeptides were increased by 8.4- and 2.9-fold in the CSF of *APP* A673T carriers as compared to controls. In total, levels of ten MAP2 phosphopeptides significantly differed ($p \leq 0.05$) between *APP* A673T carriers and controls. In the plasma from *APP* A673T carriers, the most strongly decreased protein was neprilysin (NEP), which is known as the main Aβ-degrading enzyme in the brain (Iwata et al., 2000). NEP showed a 3.5-fold decrease in *APP* A673T carrier plasma compared to controls. In the CSF, NEP was not detected. A total of 3702 proteins were detected in both CSF and plasma, but none of these were significantly differentially expressed in both CSF and plasma. In summary, we found that differentially regulated targets in the CSF and plasma samples of APP A673T carriers were, among other processes, involved in protein phosphorylation, inflammation, and mitochondrial function. Particularly in the CSF from the *APP* A673T variant carriers, we found levels of several proteins with known or suspected roles in AD to be altered.

3.3. Calcium-binding protein S100A6 and phosphatase PPP2R5B are differentially regulated in the CSF of APP A673T carriers and show inverse levels in AD brain tissue with respect to AD-associated neurofibrillary pathology

Microglial dysfunction has been shown to play an important role in AD progression (Heneka et al., 2015). Proteins secreted from glial cells are often detected in CSF (Suk, 2010). We therefore specifically assessed the markers of microglial dysfunction in our set of differentially expressed proteins in the CSF from *APP* A673T carriers as compared to controls (Fig. 3a). The soluble cleavage product of TREM2, sTREM2, has been shown to be elevated in AD CSF and is considered a marker for glial activation (Heslegrave et al., 2016). *APOE* expression has been shown to be upregulated in plaque-associated microglia (Sobue et al., 2021). Here, the CSF levels of TREM2 (reflecting most likely the CSF levels of sTREM2) or ApoE were not significantly altered in the CSF from *APP* A673T carriers. Progranulin (*GRN*) expression is increased in activated microglia and higher progranulin levels in CSF have been associated with advanced stages of AD (Suárez-Calvet et al., 2018; Mendsaikhan et al., 2019). In our proteomics analysis, progranulin displayed a trend towards decreased levels in *APP* A673T carrier CSF ($p = 0.08$). The proinflammatory cytokine, macrophage migration inhibitory factor (MIF), drivers of inflammation CD14 and FABP5, and lysosomal enzymes CTSB, CTSD, and LGALS3, which are associated with the phagocytic capacity of microglia, were not significantly altered in the CSF from *APP* A673T carriers as compared to controls (Grubman et al., 2021; Nasiri et al., 2020; Beschorner et al., 2002). Also, the CSF levels of CSF1R and its corresponding ligand CSF1, which play a central role in microglial maintenance and neuronal survival (Chitu et al., 2016), were not altered.

For further characterization and to gain insight into the general health status of the brain, we also included markers of neurodegeneration and the reactive astrocyte marker GFAP in our targeted analysis (Fig. 3b). Neurofilament subunits NEFL, NEFM, and NEFH are sensitive to neurodegeneration and their levels have been shown to be elevated in AD CSF (Hu et al., 2002; Yuan and Nixon, 2021). In the proteomics analysis of CSF, levels of the neurofilament subunits did not significantly differ between *APP* A673T carriers and controls but NEFH showed a trend towards decreased expression ($p = 0{,}21$). The levels of the neuronal marker MAP2 and astrocytic marker GFAP did not show significant differences between the sample groups. In general, most of the glial markers showed higher relative expression levels as compared to neuronal markers. This was an expected outcome as all of the study subjects were iNPH patients and microglial activation and astrogliosis have previously been associated with iNPH pathology (Eleftheriou et al., 2020; Eide and Hansson, 2018).

Fig. 3c shows relative levels of proteins with known involvement in AD progression, which were among the top 20 regulated features in the proteomics analysis of the CSF from *APP* A673T carriers. Given these findings, we analyzed RNA and protein expression of these four targets in our human post-mortem temporFal cortical sample set in relation to the degree of AD-related neurofibrillary pathology (Braak stage 0–VI) (Marttinen et al., 2019) (Fig. 3d). In the CSF from *APP* A673T carriers as compared to controls, we found a significant increase in protein levels of the phosphatase subunits PPP1CA and PPP2R5B. In the human post-mortem brain samples, the RNA levels of *PPP2R5B* were significantly decreased in Braak stage groups III + IV and V + VI as compared to Braak stage 0. RNA and protein levels of PPP1CA showed a trend

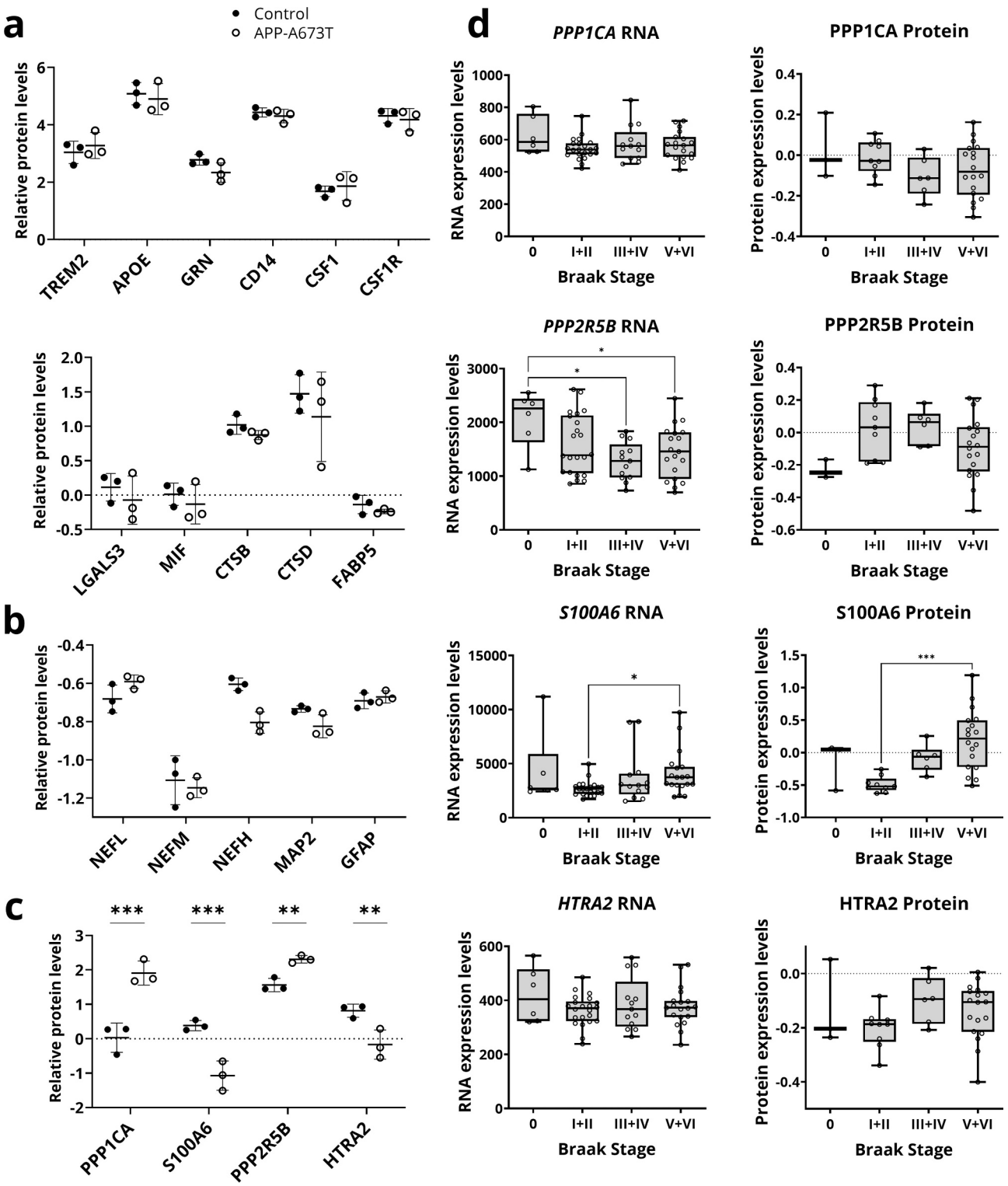

Fig. 3. Targeted analysis of protein levels in the CSF from APP A673T carriers and control individuals. a) Markers for microglial activation. b) Markers for neuronal degeneration. c) Proteomics findings in the CSF of APP A673T carriers compared to controls of targets with a known relation to AD. Relative protein levels are shown as $\log_2[\text{Sample}_{psm}/\text{Reference}_{psm}]$; PSM (peptide spectrum match). Data are shown as mean ± SD of $n = 3$. Moderated t- statistics; $^{**}p < 0.01$, $^{***}p < 0.001$. d) Expression of selected targets in the human brain in relation to AD-related neurofibrillary pathology (Braak stage 0–VI). Boxplots show median, 25th and 75th percentiles, whiskers show minimum and maximum of $n = 59$ (RNA) or $n = 36$ (protein) brain samples. Number of samples in each Braak stage 0 – V + VI group for RNA expression: $n = 6$, 22, 13, and 19, respectively. Number of samples in each Braak stage 0 – V + VI group for protein expression: n = 3, 9, 6, and 18, respectively. One-way ANOVA and Tukey's multiple comparisons test or Kruskal-Wallis and Dunn's multiple comparisons test; $^{*}p < 0.05$, $^{***}p < 0.001$.

towards a decrease with respect to AD-related neurofibrillary pathology. Levels of the calcium-binding protein S100A6 and the mitochondrial serine protease HTRA2 were significantly decreased in the CSF from *APP* A673T carriers as compared to controls. With respect to AD-related neurofibrillary pathology in human brain samples, RNA and protein levels of S100A6 significantly increased in Braak stage group V + VI as compared to Braak stage group I + II. While the RNA levels of *HTRA2* remained similar in all Braak stages, HTRA2 protein levels showed a trend towards an increase in Braak stage groups III + IV ($p = 0.2$) and V + VI ($p = 0.41$) as compared to group I + II. Collectively, the four analyzed proteins show the opposite direction of levels in post-mortem AD brain vs. the CSF of *APP* A673T carriers in comparison to the respective control groups.

In the plasma from *APP* A673T carriers, the most strongly decreased protein as compared to controls was the Aβ-degrading enzyme NEP (Table 3). To follow up on this finding, we measured NEP levels in the plasma from 47 heterozygous *APP* A673T carriers and 214 control individuals belonging to the population-based METSIM study (Fig. S 4). Plasma NEP levels in both groups showed a wide, lg-normal distribution (<0.029 ng/ml – 1569 ng/ml). Here, NEP levels were not decreased in the plasma from *APP* A673T carriers as compared to controls. As the *APOE4* allele is associated with an increased risk of developing AD and it has been shown that NEP expression differs depending on the *APOE* genotype upon neuroinflammation in a mouse model (Corder et al., 1993; Strittmatter et al., 1993; Graykowski et al., 2020), we stratified the data according to the presence (*APOE4*+) or absence (*APOE4*-) of *APOE4*. No difference was found between plasma NEP concentration from *APP* A673T carriers and controls in the *APOE4*+ or *APOE4*- group. In a previous study, we measured Aβ42 and Aβ40 levels from the same plasma samples (Martiskainen et al., 2017). Correlation analyses did not show a significant correlation between plasma NEP levels and Aβ42 ($R^2 = 0.0007$, n.s.) or Aβ40 ($R^2 = 0.0002$, n.s.), respectively. In summary, expression of the microglial activation and neuronal degeneration markers did not significantly differ in the CSF from *APP* A673T carriers as compared to controls. Calcium-binding protein S100A6 and phosphatase PPP1CA, which were differentially expressed between *APP* A673T carriers and controls, were found to show the opposite direction of expression in the post-mortem AD brain in relation to increasing neurofibrillary pathology.

3.4. Protective APP A673T variant decreases the levels of CTFβ and sAPPβ in the presence of two pathogenic AD mutations in vitro

After analyzing the effect of the protective *APP* A673T variant on APP-derived metabolite levels in the CSF of variant carriers, we next assessed *APP* A673T processing in cell culture models. We aimed particularly to assess the strength of the protective effects conveyed by the *APP* A673T variant in the presence of AD-related pathogenic changes. As an acute model, we utilized human neural cells expressing two AD causative mutations together with the APP A673T variant. To monitor long term effects on mature neurons, a 3D AD model with human neural cells cultured for 14 weeks was used (Kim et al., 2015). To generate cells expressing different types of mutant APP, the *APP* A673T variant was introduced in an internal ribosome entry site (IRES)-mediated polycistronic plasmid carrying the human APP CDS with both K670N/M671L (Swedish) and V717I (London) mutations (APP-SL) and GFP as a transfection reporter.

To evaluate the setup prior to transducing human neural cells, APP-SL and APP-SL-A673T were first overexpressed in HEK293-AP-APP (HEK) cells using transient transfection (Fig. S 5). Transfection efficiency reached >90% based on GFP-positive cells observed by fluorescence microscopy prior to cell collection. Cells transfected with a plasmid encoding GFP alone were used as a negative control for exogenous APP expression. In HEK cell lysates, the introduction of the A673T variant led to decreased levels of β-secretase-cleaved APP C-terminal fragment (CTFβ) by 50% as compared to APP-SL and a statistically significant increase in levels of α-secretase-cut APP CTF (CTFα) by 20% (Fig. S 5a). In the conditioned medium, the introduction of the *APP* A673T variant led to decreased levels of the soluble β-secretase cleavage product of APP (sAPPβ) by about 30% and Aβ42 by 10% (Fig. S 5b). Levels of sAPPα were 13% higher in cells expressing APP-SL-A673T than in those expressing APP-SL. No significant differences were detected in the levels of Aβ40 or the ratio of Aβ42/40.

Next, we expressed the same constructs in neuronal cells using lentiviral transduction. ReNcell® VM human neural progenitor (ReN) cells were transduced with APP-SL, APP-SL-A673T, or GFP alone and subsequently differentiated into neurons for 15 days. Prior to sample collection, a transduction efficiency >95% was confirmed through fluorescence microscopy.

As detected in the Western blot images (Fig. 4a), APP overexpression in ReN cells did not lead to detectable levels of APP CTFs. Therefore, γ-secretase inhibitor DAPT was used to accumulate APP CTFs in the cells. In DAPT-treated APP-SL-A673T-expressing ReN cells, levels of APPtot were slightly decreased as compared to APP-SL-expressing cells. The differences in APPtot levels were taken into account by normalizing the CTF levels to those of APPtot. In ReN cells, the introduction of the A673T variant led to decreased levels of CTFβ by 40% as compared to APP-SL despite the inhibition of γ-secretase. Consistent with the findings in HEK cells, the expression of APP-SL-A673T decreased the levels of sAPPβ by 15% and increased the levels of sAPPα by 22% in the conditioned medium of untreated ReN cells (Fig. 4b). No significant differences were seen in the medium Aβ levels or Aβ42/40 ratio.

It has been shown that overexpression of sAPPα in mouse neurons and treatment of SH-SY5Y cells with recombinant human sAPPα can lead to increased levels of inhibitory phosphorylation of GSK3β at serine 9 in the cells (Deng et al., 2015). Therefore, we assessed if the observed increase in sAPPα levels in ReN cells expressing APP-SL-A673T compared to APP-SL affected GSK3β phosphorylation. Levels of GSK3β phosphorylation did not differ between the two groups as shown by Western blot analysis (Fig. 4c). In the CSF, levels of ten MAP2 phosphopeptides significantly differed ($p \leq 0.05$) between *APP* A673T carriers and controls (Table 3). In AD patients, expression of mature MAP2 isoforms MAP2A + B was reported to dramatically decrease in the dentate gyrus, while expression of immature MAP2C was unaffected (Li et al., 2008). In ReN cells, no differences in the levels of mature or immature MAP2 isoforms were observed upon the introduction of *APP* A673T (Fig. 4c).Collectively, the analysis of APP-derived metabolite levels in 2D cell culture models expressing APP A673T together with two causative AD mutations confirmed the effectiveness of the protective *APP* A673T variant in shifting APP processing towards the non-amyloidogenic pathway.

3.5. APP A673T variant decreases the levels of sAPPβ and increases the levels of sAPPα in a 3D model of AD

So far, the impact of APP A673T expression has only been studied in 2D, short-term cell cultures. To take the chronic nature of the neuroinflammation and key pathological changes in AD, such as Aβ plaque formation and tau hyperphosphorylation into account, we introduced the APP A673T variant in a 3D in vitro model of AD (Choi et al., 2014). ReN cells were differentiated in a 3D Matrigel matrix (≈ 4 mm thickness) and cultured for 14 weeks. It has been estimated that in this model ~68% of ReN cells differentiate into neurons and ~ 30% into astrocytes (Kim et al., 2015). It has also been shown that the 3D cultures exhibit extracellular Aβ deposits and accumulate hyperphosphorylated tau after the transduction of ReN cells with the same APP-SL constructs as used in the previous experiments of this study (Fig. 4). To further elevate the deposition of Aβ, *PSEN1* with the ΔE9 mutation (PSEN1(ΔE9)) and mCherry as a reporter for viral transduction were additionally expressed in half of the cultures. To analyze the effects of the APP A673T variant, 3D cultures expressing APP-SL were compared with cultures expressing APP-SL-A673T.

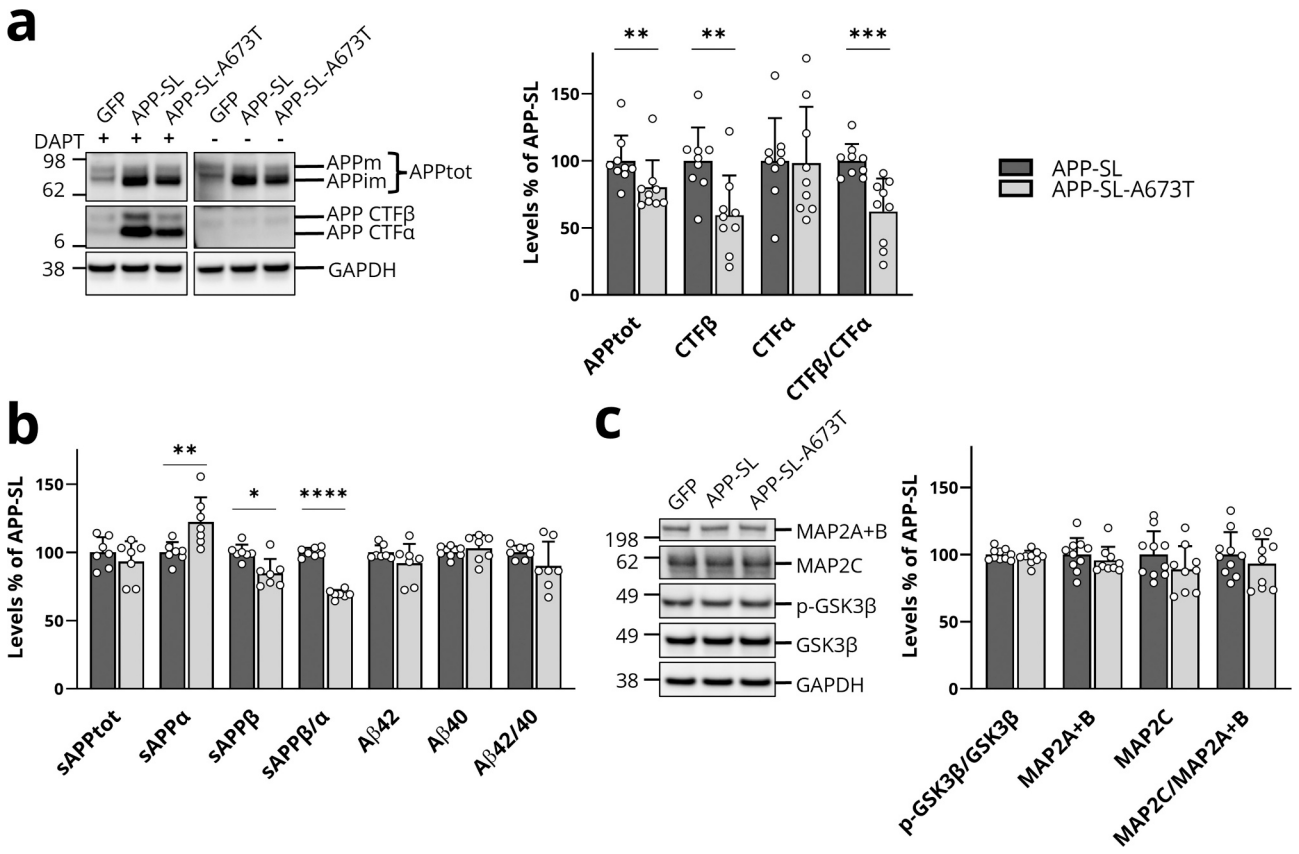

Fig. 4. Expression of APP A673T in 2D ReN cell culture model together with two pathogenic AD mutations. ReN (human neural progenitor) cells were transduced with lentivirus vectors encoding APP-SL (human APP Swedish/London pathogenic variant), APP-SL-A673T, or vector backbone. The plasmid backbone contained cytomegalovirus (CMV) promoter and GFP coding sequence separated by an internal ribosome entry side. a) Introduction of APP A673T variant decreases CTFβ levels after γ-secretase inhibition as compared to APP-SL in ReN cells. ReN cells were differentiated into neurons for 15 days prior to treatments and collection. A subset of the cells was treated with 1 μM γ-secretase inhibitor DAPT for 24 h to detect the APP CTFs. Levels of APP CTFs CTFβ and CTFα were normalized to sAPPtot levels. b) Introduction of APP A673T variant increases sAPPα levels and decreases sAPPβ levels as compared to APP-SL in ReN cells. All levels were measured by ELISA and normalized to sAPPtot levels. c) No changes in the phosphorylation of GSK3β at serine 9 or levels of the neuronal target MAP2 were observed in ReN cells over-expressing APP-SL compared to APP-SL-A673T. Levels of the MAP2 high-molecular-mass isoforms MAP2A and MAP2B and the low-molecular-mass isoform MAP2C were normalized to GAPDH. All Data are shown as mean + SD of $n = 7$–10 of two independent experiments. Independent samples *t*-test or independent samples Mann Whitney *U* test; *$p < 0.05$, ** $p < 0.01$, *** $p < 0.001$, ****$p < 0.0001$.

The most prominent change in the 3D model of AD upon the introduction of the APP A673T variant was an increase in sAPPα levels in the conditioned medium by ~35% (Fig. 5a). This increase in the sAPPα levels was observed both with and without co-expression of *PSEN1* (ΔE9). At the same time, sAPPβ levels were decreased by ~10% in the 3D cultures expressing APP-SL-A673T as compared to APP-SL. As expected, co-expression of *PSEN1*(ΔE9) strongly increased the ratio of Aβ42/Aβ40. In the 3D culture lysates, the levels of CTFβ could not be detected by Western blotting and the CTFα levels were unaltered upon introduction of the protective APP variant (Fig. 5b). Similar to the results in 2D ReN cell cultures, the levels of GSK3β phosphorylation or MAP2 isoforms did not significantly differ between APP-SL and APP-SL-A673T-expressing 3D cultures. In summary, the introduction of the APP A673T variant together with AD causative mutations in different cell culture models emphasized the strength of the protective variant. Even in the presence of the pathogenic *APP* mutations, the introduction of the protective variant shifted APP processing towards the non-amyloidogenic pathway. The most prominent and consistent change in the 2D and 3D cell cultures expressing APP-SL-A673T compared to APP-SL was a decrease in sAPPβ levels and an increase in sAPPα levels. Similar changes were detected when comparing the CSF samples from *APP* A673T carriers with those from the controls.

4. Discussion

Understanding the molecular basis by which the APP A673T variant confers protection against AD to its carriers can contribute to both a better understanding of AD pathogenesis and designing effective therapeutic strategies (Harper et al., 2015). With the present study, we provide the first insight into global protein expression changes in the CSF of APP A673T variant carriers. Additionally, we confirmed the strong protective effects of the APP A673T variant against the development of AD-associated pathologies in the variant carriers and in vitro models.

In the Finnish EADB sample set, we found the protective APP A673T allele in 13 out of 2109 aged subjects. The resulting allele frequency of 0.3% lies in between the frequencies found in the previous studies in Finnish cohorts, where allele frequencies of 0.1, 0.3, and 0.5% have been found in two population-based and one schizophrenia cohort, respectively (Muratore et al., 2014; Strittmatter et al., 1993; Corder et al., 1994). In accordance with what was observed in the Icelandic population (Jonsson et al., 2012), we found that the APP A673T variant was significantly more common in the Finnish elderly control group than in the AD group, confirming the protective effect of A673T variant. Furthermore, AD-related pathological changes were absent in the three frontal cortical biopsies from iNPH patients carrying APP A673T variant. In the previous studies of iNPH patients, Aβ pathology has been

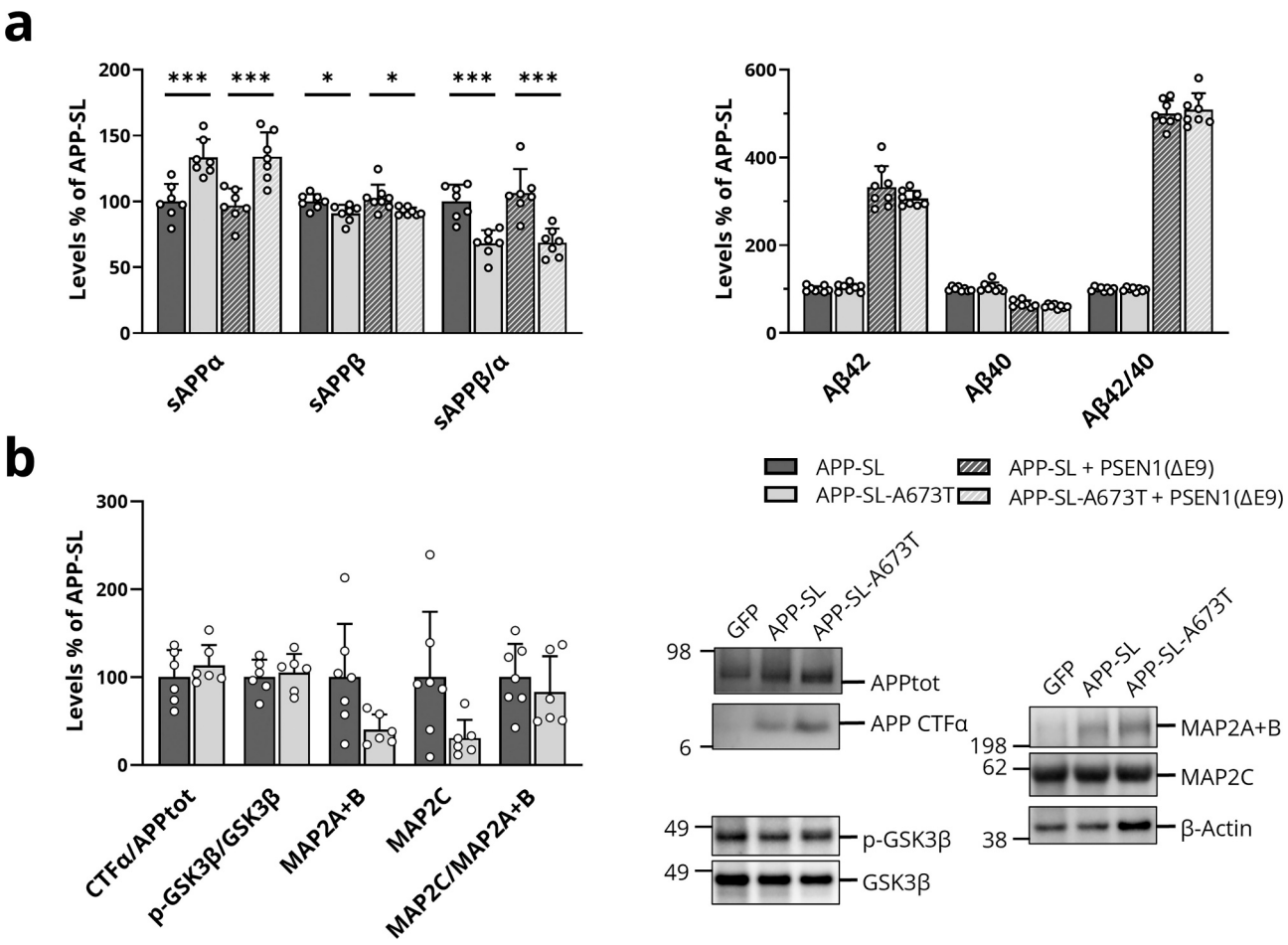

Fig. 5. Introduction of the APP A673T variant into a 3D model of AD. ReN cells were transduced with lentiviral vectors encoding APP-SL (human APP Swedish/London pathogenic variant), APP-SL-A673T, or vector backbone. The plasmid backbone contained cytomegalovirus (CMV) promoter and GFP coding sequence separated by an internal ribosome entry side. Part of the cells were co-transduced with vectors encoding *PSEN1*(ΔE9) (human presenilin 1 exon 9 deletion pathogenic variant) along with mCherry, separated by an internal ribosome entry side. The cells were differentiated in a 3D Matrigel matrix (≈4 mm thickness) and cultured for 14 weeks prior to collection. a) Introduction of APP A673T variant increases sAPPα levels and decreases sAPPβ levels in a 3D model of AD utilizing expression of APP-SL or APP-SL together with *PSEN1*(ΔE9). Levels of Aβ were not altered upon the introduction of the protective APP A673T variant. All levels were measured by ELISA and normalized to sAPPtot levels. b) No significant changes in APP C-terminal fragment CTFα, phosphorylation of GSK3β at serine 9, or levels of the neuronal target MAP2 were observed in ReN cells overexpressing APP-SL compared to APP-SL-A673T. Levels of the MAP2 high-molecular-mass isoforms MAP2A and MAP2B and the low-molecular-mass isoform MAP2C were normalized to β-actin. All data are shown as mean + SD of $n = 7$–10 of two independent experiments. Independent samples *t*-test or independent samples Mann Whitney *U* test; $^{*}p < 0.05$, $^{***}p < 0.001$.

reported to be present in 42% of the studied subjects in the Kuopio iNPH sample set (Leinonen et al., 2012), while 68% showed evidence for at least one AD pathological marker in another study (Hamilton et al., 2010). Correspondingly, an increased occurrence of clinical AD has been observed in iNPH patients as compared to the general population (Luikku et al., 2019). The absence of Aβ and p-tau in the biopsies of the iNPH patients carrying APP A673T variant further supports the hypothesis of a protective effect of this variant against AD-related pathology.

In contrast to plasma, CSF is in direct contact with the brain and has been shown to provide a more accurate estimate than plasma samples for biochemical changes in the brain (Panyard et al., 2021; Mehta et al., 2000). By analyzing the levels of AD pathology-related peptides in the CSF of APP A673T variant carriers as compared to control samples, we found that the protective variant associated with significantly lower levels of sAPPβ and Aβ42. Moreover, the CSF levels of Aβ40 were reduced in the APP A673T variant carriers, although this result did not reach statistical significance. Consequently, the ratio of Aβ42/Aβ40 was not significantly altered alongside the unaltered CSF levels of sAPPtot, sAPPα, p-tau and t-tau. In the CSF of AD patients, Aβ42 is generally found in lower levels than in cognitively normal individuals, probably reflecting deposition of Aβ in the brain (Blennow et al., 2010). As Aβ pathology was absent in the biopsies of the iNPH patients, it is unlikely that low CSF Aβ42 levels are caused by brain Aβ deposition in APP A673T variant carriers. A decrease in sAPPβ levels was also observed in the 3D model of AD upon the introduction of APP A673T variant, indicating that the protective variant modulates BACE1 cleavage of APP. Further supporting the idea that the APP A673T variant might affect BACE1 cleavage of APP were the findings related to the significantly decreased CTFβ levels in APP-SL-A673T-expressing cells as compared to APP-SL after inhibition of γ-secretase. Previous studies related to the expression of wild-type APP with respect to APP A673T variant in different cell types and in vitro enzyme activity assays have proposed different effects of the APP A673T variant on APP processing as the main mechanism for its protection against AD. In accordance with our findings, several studies found a reduction in BACE1 cleavage of APP due to the A673T variant and suggested a modulation of the catalytic turnover rate of APP by BACE1 (Jonsson et al., 2012; Maloney et al., 2014). Other studies proposed a reduction in the γ-secretase-mediated cleavage of APP A673T based on the findings that CTFβ levels were unaltered between cells expressing WT APP and APP A673T and that expression of CTFβ carrying A673T led to a decrease in Aβ production as compared to

WT CTFβ (Kimura et al., 2016; Kokawa et al., 2015). Studies focusing on the properties of Aβ carrying A2T (corresponding to A673T site in APP) have proposed that N-terminal fragments of Aβ A2T of various lengths can retard or delay aggregation of WT Aβ (Benilova et al., 2014; Lin et al., 2017). Furthermore, Aβ40 A2T peptides have been shown to differentially affect mitochondrial trafficking in primary cortical mouse neurons. Moreover, their plasma membrane binding and internalization into neurons were reduced as compared to WT Aβ40 (Zhang et al., 2018). In summary, these results suggest that the APP A673T variant conveys protection against AD pathology through an interplay of multiple factors, such as modulating the generation of different APP-derived peptides by the secretases as well as their molecular function by altering the conformation of some of the generated peptides.

One possible way how altered levels or conformational states of APP proteolytic products can contribute to the protective effect of APP A673T variant is by evoking expressional changes of downstream targets. It has previously been shown that Aβ and APP intracellular fragment (AICD) can directly alter gene expression by acting as transcription factor (Multhaup et al., 2015; Słomnicki and Leśniak, 2008; Maloney and Lahiri, 2011). Furthermore, also other APP-derived peptides, such as CTFs and sAPP, indirectly regulate gene expression e.g. through interaction with adapter proteins (Schettini et al., 2010; Ryan et al., 2013; Li et al., 2010). Here, we looked at differential (phospho)peptide expression in the CSF and plasma of APP A673T variant carriers as compared to controls and found that processes related to protein phosphorylation were significantly over-represented in the differentially expressed peptides in the CSF and plasma of the protective variant carriers. Aberrant protein phosphorylation through dysregulation of kinases and phosphatases has been identified as a critical step in AD pathogenesis and progression (Perluigi et al., 2016). The most prominent example of an imbalance between the activity of kinases and phosphatases in AD is the hyperphosphorylation of tau (Goedert et al., 1991; Gong et al., 1995). In AD brain, the activity and/or expression of protein phosphatases-1 (PP1), −2A (PP2A), −5 (PP5), and PTEN have shown to be decreased (Griffin et al., 2005; Gong et al., 1993; Gong et al., 2004). A central role in the phosphorylation of tau has been attributed to PP2A, which most efficiently released phosphate from hyperphosphorylated tau in vitro. Supporting this notion, inhibition of PP2A was shown to induce tau hyperphosphorylation in vivo in the rat brain (Wang et al., 1996; Tian et al., 2004; Martin et al., 2013). Here, protein levels of the PP2A regulatory subunit PPP2R5B were found to be increased in the CSF from APP A673T carriers as compared to controls, which is opposite to the finding on the expression of PPP2R5B RNA in the post-mortem AD brain samples with advanced tau pathology. These findings support the important role of PP2A in AD disease progression and suggest that the protective APP A673T variant may positively influence PP2A function and subsequently, reduce the phosphorylation of tau. Levels of PPP1CA, a subunit of PP1, which is also involved in tau dephosphorylation, were increased in the CSF of the APP A673T variant carriers by 3.6-fold, suggesting further positive regulatory effects of the protective variant on the dephosphorylation of tau. In the AD brain, PPP1CA levels are reduced and it has been suggested that this reduction is mediated through microRNA (miR)-125b, which is elevated in AD (Banzhaf-Strathmann et al., 2014). In primary hippocampal rat neurons, overexpression of miR-125b caused tau hyperphosphorylation, while overexpression of PPP1CA prevented miR-125b-induced tau phosphorylation (Banzhaf-Strathmann et al., 2014). Thus, future studies should be focused on assessing whether the miR-125b-mediated regulation is involved in the observed increase of PPP1CA levels in the CSF of the APP A673T variant carriers. PP5, the third phosphoprotein phosphatase (PPP) dysregulated in AD, has been shown to interact with the calcium-binding protein S100A6, which was strongly reduced in the CSF from APP A673T carriers in this study. Interestingly, S100A6 was identified as one of the positively correlated proteins with AD disease phenotype, and S100A6 accumulates in the center of Aβ plaques and the surrounding astrocytes (Wruck et al., 2016; Hagmeyer et al., 2019; Boom et al., 2004). Here, we confirmed the increase in S100A6 levels in post-mortem brain samples in relation to increased AD-related neurofibrillary pathology. Counterintuitively to the observed expression pattern of S100A6, it has been shown that S100A6 enhances the phosphatase activity of PPP5C towards phosphorylated tau protein and that S100A6 delayed Aβ42 aggregation in in vitro kinetic experiments, suggesting that increased levels of S100A6 in the brain could exert protective effects in terms of AD-related pathology (Hagmeyer et al., 2019; Haldar et al., 2020). Conceivably, the increase in S100A6 expression in AD brains might be a compensatory protective effect. There are indications for the involvement of APP in the regulation of S100A6 expression. At the transcriptional level, the *S100A6* gene promoter has been shown to be activated by β-catenin, which again can physically bind to APP, as shown in APP-overexpressing N2a cells, and thereby, excluded from the nucleus (Kilańczyk et al., 2012; Zhang et al., 2018). An involvement of APP in the regulation of S100A6 expression is supported by our finding that S100A6 expression appears to be altered in APP A673T variant carriers.

Mitochondrial oxidative stress in microglia has previously been linked to the development of AD (Agrawal and Jha, 2020), and the Aβ40 A2T peptide has been shown to differentially affect mitochondrial trafficking as compared to WT Aβ40 (Zhang et al., 2018). Here, processes important for mitochondrial function were found to be over-represented among the differentially expressed peptides in the CSF and plasma samples. We found that HTRA2 protein levels were reduced in the CSF from APP A673T variant carriers as compared to controls. HTRA2 is a mitochondrial serine protease and in in vitro assays, HTRA2 significantly delayed the aggregation of Aβ42 peptides (Kooistra et al., 2009). Functional analyses indicated a significant increase in HTRA activity in the AD brain (Darreh-Shori et al., 2019; Westerlund et al., 2011) and a HTRA2 inhibitor has been reported to exert neuroprotection in rats (Su et al., 2009).

Some of the proteins that were found to be differentially expressed in the CSF and plasma of APP A673T variant carriers were involved in processes related to inflammatory cell response. One of these was HAVCR2, which showed decreased levels in the CSF of protective variant carriers. HAVCR2 (also named TIM-3) has been shown to regulate inflammatory mediators in microglia and mediate microglial toxicity (Wang, and wei, Zhu X li, Qin L ming, Qian H jun, Wang Y., 2015). Interestingly, *HAVCR2* came up as one of the seven new AD risk loci in a recent genome-wide association study (Wightman et al., 2021), suggesting a role for the protein in AD pathogenesis. Targeted analysis of the proteomics data from the CSF of APP A673T variant carriers revealed a trend towards a decrease in proteins, which promote chronic inflammation, but no significant expressional changes were found in known markers of neuroinflammation, such as MIF, CD14, and FABP5. Analysis of phosphopeptide expression in the CSF samples revealed phospho site-specific changes in several AD-associated proteins, but the impact of these protein modifications is for the most part difficult to interpret.

Even though NEP levels were found to be strongly decreased in the plasma from APP A673T variant carriers as compared to controls, we were not able to confirm this decrease in APP A673T variant carriers from the population-based METSIM cohort. We have previously shown in the METSIM cohort on the average 28% lower plasma levels of Aβ40 and Aβ42 in APP A673T variant carriers as compared to control individuals (Kimura et al., 2016) and thus, this cohort was used to assess the levels of plasma NEP and the potential correlation of NEP levels with Aβ by considering also the *APOE* status. Several studies have reported that NEP gene expression is upregulated through the binding of AICD to its promoter region, where AICD generated via the amyloidogenic pathway appeared to be involved in the regulation of NEP expression (Belyaev et al., 2009; Grimm et al., 2015). In the analysis of plasma samples, there were remarkably great differences in the NEP concentration between different individuals, which complicated the analysis of the data. A large interindividual variation in plasma NEP concentration

has been observed in another study as well (Prausmüller et al., 2020). There might be other factors affecting NEP levels in the plasma, masking the potential effects of the APP A673T variant. When interpreting the results of both CSF and plasma analysis, also the small number of cases must be taken into account. Importantly, the small sample size most likely also explains the relatively low number of targets that were showing significantly different levels and consequently, it is probably the reason for a missing overlap in the equally regulated targets between CSF and plasma samples. However, given that APP A673T is a rare variant and almost exclusively found in Northern European populations, it is difficult to acquire larger sizes of CSF or brain biopsy samples from variant carriers. Another factor to be considered is that the studied APP A673T variant carriers have an underlying diagnosis of iNPH. The impact of this factor on the comparison of APP A673T variant carriers and non-carriers was minimized by choosing the control individuals also from the iNPH patient group. Furthermore, as described previously, the levels of sAPP and Aβ differed significantly between iNPH patients and healthy controls (Moriya et al., 2015). This was the main reason why carefully matched CSF samples obtained from the iNPH patient cohort were used as controls in the present study instead of healthy controls to address the effects of the protective A673T variant without having the confounding effects related to iNPH disease itself.

The results from our cell culture experiments were consistent with previous studies, showing that the introduction of the APP A673T variant decreased the levels of Aβ42 in HEK cells (Jonsson et al., 2012; Maloney et al., 2014). In the present study, this was detected even in the presence of the causative Swedish and London mutations, indicating the strong potency of the protective variant to modulate APP processing. Mutant *APP* carrying the Swedish and/or London mutations has been utilized to generate commonly used mouse models of AD (Jankowsky and Zheng, 2017). In this study, we chose to introduce these mutations together with the *APP* A673T variant due to their suitability to model important features of AD as demonstrated in the different mouse and 3D cell culture models (Kim et al., 2015; Jankowsky and Zheng, 2017). In both 2D and 3D cultures of the ReN cells, we did not observe an effect of the APP A673T variant on Aβ levels, even though the levels of sAPPα and sAPPβ were altered. A recent study explored the effect of APP A673T insertion in APP constructs harboring 29 different AD causative mutations (Guyon et al., 2020). The study used Aβ42 and Aβ40 in the SH-SY5Y cell-conditioned medium as a measure of the protective effects conveyed by the APP A673T variant and showed that Aβ levels were decreased for some of the AD causative mutations upon introduction of APP A673T (Guyon et al., 2020). Our results suggest that the levels of sAPPα and sAPPβ might serve as a more reliable measure of the protective effect conferred by the protective APP A673T variant.

So far, the reduced production of Aβ from the APP A673T variant has received the most attention. Our results from both CSF and cell culture analyses suggest focusing on the altered production of sAPPα and sAPPβ as well. In the CSF of AD patients and patients with MCI due to AD, increased levels of sAPPα and sAPPβ have been found as compared to controls (Araki et al., 2017; Araki et al., 2022). Other studies have detected unaltered CSF levels of sAPPα and/or sAPPβ from AD patients as compared to healthy controls (Brinkmalm et al., 2013; Savage et al., 2015). Similarly, Dobrovska et al. did not observe a significant difference in the CSF levels of sAPPα and sAPPβ between AD patients and age-matched controls (Dobrowolska et al., 2014). However, this study detected an increase in the ratio of sAPPβ/sAPPα in the AD group, indicating a shift towards amyloidogenic processing of APP leading to very subtle changes in the CSF levels of sAPP. Therefore, the ratio of sAPPβ/sAPPα could be considered a better CSF marker for AD-related changes in APP processing. Consistent with this notion, the CSF ratio of sAPPβ/sAPPα was decreased in the protective APP A673T carries, although this result did not reach statistical significance.

Many neuroprotective functions have been attributed to sAPPα, conveyed through modulation of PI3K, MAPK, and GSK3β signaling pathways among others (Dar and Glazner, 2020). It has been shown that sAPPα itself can act as an inhibitor of BACE1, while CTFα is capable of inhibiting γ-secretase (Deng et al., 2015; Peters-Libeu et al., 2015; Obregon et al., 2012; Tian et al., 2010). Those might be feedback mechanisms, which when dysregulated may contribute to AD pathogenesis. In the past, amyloidogenic processing has been the main target of drug development against AD, while targeting the α-secretase cleavage of APP might hold therapeutic potential as well (Habib et al., 2017; Lichtenthaler, 2011; Fahrenholz and Postina, 2006; Zhao et al., 2020). Clinical trials with drugs, which inhibit BACE1, have failed so far. One of the reasons for the failure may be that the numerous other substrates of BACE1 are needed for essential neuronal functions (Hampel et al., 2021). Nevertheless, the reduction of sAPPβ levels observed in the CSF from APP A673T carriers indicates that a reduction in the β-cleavage of APP might still hold protective potential against AD, but the reduction in BACE1 activity might need to be very subtle or only limited to APP as a substrate. In a recent study, a short peptide generated from sAPPα was designed, which specifically binds to BACE1 at the BACE1-APP cleavage site and reduced Aβ production in vivo and in vitro (Lai et al., *2022*). Other studies have explored the possibility of editing APP through the insertion of the A673T variant as a future treatment option for AD caused by dominantly inherited causative variants. However, the establishment of genome-editing therapies against neurological disorders still requires a great amount of research and development (Guyon et al., 2020; Guyon et al., 2021; Duarte and Déglon, 2020).

5. Conclusions

Taken together, we now here show for the first time that the APP A673T variant significantly reduces sAPPβ and Aβ42 levels in human CSF. Furthermore, we found that several AD-associated proteins were differentially expressed in the CSF and plasma of APP A673T variant carriers as compared to matched controls, including several proteins involved in tau dephosphorylation. In 2D and 3D cell culture models, the introduction of the APP A673T variant modulated the levels of several APP cleavage products and shifted APP processing towards the non-amyloidogenic processing pathway even in the presence of two pathogenic APP variants. Collectively, our findings emphasize that the drug development processes should not concentrate on Aβ reduction or BACE1 inhibition alone but reinforce the focus on a more holistic approach targeting different steps of APP processing and downstream targets. Future analyses of APP A673T variant carrier biofluids from much larger sample sets and the subsequent comparison with different data from APP A673T variant carriers might profoundly contribute to the identification of specific proteins and pathways, which play an active role in AD progression and could be utilized as early AD biomarkers or drug targets.

Ethics approval and consent to participate

The study was approved by the Hospital District of Northern Savo Ethics Committee. Written informed consent was obtained from all subjects included in this study.

Availability of data and materials

The datasets used analyzed during the current study are available from the corresponding author on reasonable request.

Funding

This research was supported by Academy of Finland (grant numbers 338182, 307866, 315459, and 330178, 339767); Sigrid Jusélius Foundation; the Strategic Neuroscience Funding of the University of Eastern Finland; the Alfred Kordelin Foundation; the Finnish Brain Foundation; the Orion Research Foundation sr; Kuopio University Hospital VTR Fund. This project is co-funded by the Horizon 2020 Framework

Program of the European Union (Marie Skłodowska Curie grant agreement No 740264).

Authors' contributions

Rebekka Wittrahm: Conceptualization, Methodology, Formal analysis, Writing – Original Draft, Visualization, Investigation, Funding acquisition. **Mari Takalo:** Conceptualization, Methodology, Formal analysis, Writing – Original Draft, Supervision, Investigation, Project administration, Funding acquisition. **Teemu Kuulasmaa:** Software, Investigation, Formal analysis. **Petra M Mäkinen:** Investigation. **Petri Mäkinen:** Investigation. **Saša Končarević:** Investigation, Formal analysis. **Vadim Fartzdinov:** Investigation, Formal analysis. **Stefan Selzer:** Investigation, Formal analysis. **Tarja Kokkola:** Supervision, Formal analysis, Writing – Review & Editing. **Leila Antikainen:** Investigation. **Henna Martiskainen:** Supervision, Writing – Review & Editing. **Susanna Kemppainen:** Supervision, Writing – Review & Editing. **Mikael Marttinen:** Formal analysis, Writing – Review & Editing. **Heli Jeskanen:** Supervision, Writing – Review & Editing. **Hannah Rostalski:** Supervision, Writing – Review & Editing. **Eija Rahunen:** Investigation. **Miia Kivipelto:** Resources. **Tiia Ngandu:** Resources. **Teemu Natunen:** Supervision, Writing – Review & Editing. **Jean-Charles Lambert:** Resources. **Rudolph E Tanzi:** Supervision, Resources. **Doo Yeon Kim:** Supervision, Resources. **Tuomas Rauramaa:** Investigation, Resources. **Sanna-Kaisa Herukka:** Project administration, Resources. **Hilkka Soininen:** Resources. **Markku Laakso:** Resources. **Ian Pike:** Resources, Project administration. **Ville Leinonen:** Supervision, Project administration, Resources, Funding acquisition. **Annakaisa Haapasalo:** Conceptualization, Methodology, Supervision, Writing – Original Draft, Funding acquisition. **Mikko Hiltunen:** Conceptualization, Methodology, Supervision, Formal analysis, Writing – Original Draft, Project administration, Funding acquisition.

Declaration of Competing Interest

The authors declare that they have no competing interests.

Data availability

Data will be made available on request.

Acknowledgments

We thank Biocenter Kuopio National Virus Vector Laboratory at the University of Eastern Finland (Kuopio, Finland) for packaging of the lentiviral vectors and the University of Eastern Finland Cell and Tissue Imaging Unit (Kuopio, Finland), supported by Biocenter Kuopio and Biocenter Finland, for maintenance and help with the microscopes. We also thank Gitte Böhm and Jutta Korder for running sample preparation for LC-MS-experiments, Stephan Jung, Antje Berfelde, and Claudia Höhle for running the LC-MS-analyses, Michael Bremang for computational proteomics and assistance in the preparation of the manuscript, Juliane Weisser for assistance in the preparation of the manuscript.

Appendix A. Supplementary data

Supplementary data to this article can be found online at https://doi.org/10.1016/j.nbd.2023.106140.

References

Agrawal, I., Jha, S., 2020. Mitochondrial dysfunction and Alzheimer's disease: role of microglia. Front. Aging Neurosci. 12, 252.

Araki, W., Hattori, K., Kanemaru, K., Yokoi, Y., Omachi, Y., Takano, H., et al., 2017 Sep 22. Re-evaluation of soluble APP-α and APP-β in cerebrospinal fluid as potential biomarkers for early diagnosis of dementia disorders. Biomarker Res. 5 (1), 28.

Araki, W., Kanemaru, K., Hattori, K., Tsukamoto, T., Saito, Y., Yoshida, S., et al., 2022 Feb. Soluble APP-α and APP-β in cerebrospinal fluid as potential biomarkers for differential diagnosis of mild cognitive impairment. Aging Clin. Exp. Res. 34 (2), 341–434.

Banzhaf-Strathmann, J., Benito, E., May, S., Arzberger, T., Tahirovic, S., Kretzschmar, H., et al., 2014 Aug 1. MicroRNA-125b induces tau hyperphosphorylation and cognitive deficits in Alzheimer's disease. EMBO J. 33 (15), 1667–1680.

Bellenguez, C., Küçükali, F., Jansen, I.E., Kleineidam, L., Moreno-Grau, S., Amin, N., et al., 2022 Apr 4. New insights into the genetic etiology of Alzheimer's disease and related dementias. Nat. Genet. 1–25.

Belyaev, N.D., Nalivaeva, N.N., Makova, N.Z., Turner, A.J., 2009 Jan. Neprilysin gene expression requires binding of the amyloid precursor protein intracellular domain to its promoter: implications for Alzheimer disease. EMBO Rep. 10 (1), 94–100.

Benilova, I., Gallardo, R., Ungureanu, A.A., Castillo Cano, V., Snellinx, A., Ramakers, M., et al., 2014 Nov 7. The Alzheimer disease protective mutation A2T modulates kinetic and thermodynamic properties of amyloid-β (Aβ) aggregation. J. Biol. Chem. 289 (45), 30977–30989.

Benjamini, Y., Hochberg, Y., 1995. Controlling the false discovery rate: a practical and powerful approach to multiple testing. J. R. Stat. Soc. Ser. B Methodol. 57 (1), 289–300.

Bernstein, S.L., Dupuis, N.F., Lazo, N.D., Wyttenbach, T., Condron, M.M., Bitan, G., et al., 2009 Jul 1. Amyloid-β protein oligomerization and the importance of tetramers and dodecamers in the aetiology of Alzheimer's disease. Nat. Chem. 1 (4), 326–331.

Beschorner, R., Nguyen, T.D., Gözalan, F., Pedal, I., Mattern, R., Schluesener, H.J., et al., 2002 Jun. CD14 expression by activated parenchymal microglia/macrophages and infiltrating monocytes following human traumatic brain injury. Acta Neuropathol. 103 (6), 541–549.

Bhattacharyya, R., Barren, C., Kovacs, D.M., 2013 Jul 3. Palmitoylation of amyloid precursor protein regulates Amyloidogenic processing in lipid rafts. J. Neurosci. 33 (27), 11169–11183.

Blennow, K., Hampel, H., Weiner, M., Zetterberg, H., 2010 Mar. Cerebrospinal fluid and plasma biomarkers in Alzheimer disease. Nat. Rev. Neurol. 6 (3), 131–144.

Boom, A., Pochet, R., Authelet, M., Pradier, L., Borghgraef, P., Van Leuven, F., et al., 2004 Dec 6. Astrocytic calcium/zinc binding protein S100A6 over expression in Alzheimer's disease and in PS1/APP transgenic mice models. Biochim. Biophys. Acta 1742 (1–3), 161–168.

Borchelt, D.R., Thinakaran, G., Eckman, C.B., Lee, M.K., Davenport, F., Ratovitsky, T., et al., 1996 Nov. Familial Alzheimer's disease-linked presenilin 1 variants elevate Abeta1-42/1-40 ratio in vitro and in vivo. Neuron. 17 (5), 1005–1013.

Brinkmalm, G., Brinkmalm, A., Bourgeois, P., Persson, R., Hansson, O., Portelius, E., et al., 2013 Jun 4. Soluble amyloid precursor protein α and β in CSF in Alzheimer's disease. Brain Res. (1513), 117–126.

Chitu, V., Gokhan, Ş., Nandi, S., Mehler, M.F., Stanley, E.R., 2016 Jun. Emerging roles for CSF-1 receptor and its ligands in the nervous system. Trends Neurosci. 39 (6), 378–393.

Choi, S.H., Kim, Y.H., Hebisch, M., Sliwinski, C., Lee, S., D'Avanzo, C., et al., 2014 Nov. A three-dimensional human neural cell culture model of Alzheimer's disease. Nature. 515 (7526), 274–278.

Corder, E.H., Saunders, A.M., Risch, N.J., Strittmatter, W.J., Schmechel, D.E., Gaskell, P. C., et al., 1994 Jun. Protective effect of apolipoprotein E type 2 allele for late onset Alzheimer disease. Nat. Genet. 7 (2), 180–184.

Corder, E.H., Saunders, A.M., Strittmatter, W.J., Schmechel, D.E., Gaskell, P.C., Small, G. W., et al., 1993 Aug 13. Gene dose of apolipoprotein E type 4 allele and the risk of Alzheimer's disease in late onset families. Science. 261 (5123), 921–923.

Crook, R., Verkkoniemi, A., Perez-Tur, J., Mehta, N., Baker, M., Houlden, H., et al., 1998 Apr. A variant of Alzheimer's disease with spastic paraparesis and unusual plaques due to deletion of exon 9 of presenilin 1. Nat. Med. 4 (4), 452–455.

Dar, N.J., Glazner, G.W., 2020. Jun. Deciphering the neuroprotective and neurogenic potential of soluble amyloid precursor protein alpha (sAPPα). Cell. Mol. Life Sci. 77 (12), 2315–2330.

Darreh-Shori, T., Rezaeianyazdi, S., Lana, E., Mitra, S., Gellerbring, A., Karami, A., et al., 2019 Jul. Increased active OMI/HTRA2 serine protease displays a positive correlation with cholinergic alterations in the Alzheimer's disease brain. Mol. Neurobiol. 56 (7), 4601–4619.

Dayon, L., Turck, N., Kienle, S., Schulz-Knappe, P., Hochstrasser, D.F., Scherl, A., et al., 2010 Feb 1. Isobaric tagging-based selection and quantitation of cerebrospinal fluid tryptic peptides with reporter calibration curves. Anal. Chem. 82 (3), 848–858.

Deng, J., Habib, A., Obregon, D.F., Barger, S.W., Giunta, B., Wang, Y.J., et al., 2015 Nov. Soluble amyloid precursor protein alpha inhibits tau phosphorylation through modulation of GSK3β signaling pathway. J. Neurochem. 135 (3), 630–637.

Dobrowolska, J.A., Kasten, T., Huang, Y., Benzinger, T.L.S., Sigurdson, W., Ovod, V., et al., 2014 Mar 19. Diurnal patterns of soluble amyloid precursor protein metabolites in the human central nervous system. PLoS One 9 (3), e89998.

Duarte, F., Déglon, N., 2020. Genome editing for CNS disorders. Front. Neurosci. 14 [cited 2022 Feb 2]. Available from: https://doi.org/10.3389/fnins.2020.579062 [cited 2022 Feb 2]. Available from:

Eide, P.K., Hansson, H.A., 2018 Aug. Astrogliosis and impaired aquaporin-4 and dystrophin systems in idiopathic normal pressure hydrocephalus. Neuropathol. Appl. Neurobiol. 44 (5), 474–490.

Eleftheriou, A., Blystad, I., Tisell, A., Gasslander, J., Lundin, F., 2020 Apr 9. Indication of Thalamo-cortical circuit dysfunction in idiopathic Normal pressure hydrocephalus: a diffusion tensor imaging study. Sci. Rep. 10 (1), 6148.

Fahrenholz, F., Postina, R., 2006. Alpha-secretase activation–an approach to Alzheimer's disease therapy. Neurodegener. Dis. 3 (4–5), 255–261.

Gatz, M., Reynolds, C.A., Fratiglioni, L., Johansson, B., Mortimer, J.A., Berg, S., et al., 2006 Feb 1. Role of genes and environments for explaining Alzheimer disease. Arch. Gen. Psychiatry 63 (2), 168–174.
Goate, A., Chartier-Harlin, M.C., Mullan, M., Brown, J., Crawford, F., Fidani, L., et al., 1991 Feb 21. Segregation of a missense mutation in the amyloid precursor protein gene with familial Alzheimer's disease. Nature. 349 (6311), 704–706.
Goedert, M., Spillantini, M.G., Crowther, R.A., 1991 Jul. Tau proteins and neurofibrillary degeneration. Brain Pathol. 1 (4), 279–286.
Gong, C.X., Liu, F., Wu, G., Rossie, S., Wegiel, J., Li, L., et al., 2004 Jan. Dephosphorylation of microtubule-associated protein tau by protein phosphatase 5. J. Neurochem. 88 (2), 298–310.
Gong, C.X., Shaikh, S., Wang, J.Z., Zaidi, T., Grundke-Iqbal, I., Iqbal, K., 1995. Phosphatase activity toward abnormally phosphorylated τ: decrease in Alzheimer disease brain. J. Neurochem. 65 (2), 732–738.
Gong, C.X., Singh, T.J., Grundke-Iqbal, I., Iqbal, K., 1993 Sep. Phosphoprotein phosphatase activities in Alzheimer disease brain. J. Neurochem. 61 (3), 921–927.
Graykowski, D., Kasparian, K., Caniglia, J., Gritsaeva, Y., Cudaback, E., 2020 Jul 4. Neuroinflammation drives APOE genotype-dependent differential expression of neprilysin. J. Neuroimmunol. (346), 577315
Griffin, R.J., Moloney, A., Kelliher, M., Johnston, J.A., Ravid, R., Dockery, P., et al., 2005 Apr. Activation of Akt/PKB, increased phosphorylation of Akt substrates and loss and altered distribution of Akt and PTEN are features of Alzheimer's disease pathology. J. Neurochem. 93 (1), 105–117.
Grimm, M., Mett, J., Stahlmann, C., Grösgen, S., Haupenthal, V., Blümel, T., et al., 2015. APP intracellular domain derived from amyloidogenic β- and γ-secretase cleavage regulates neprilysin expression. Front. Aging Neurosci. 7 [cited 2022 Feb 7]. Available from: https://doi.org/10.3389/fnagi.2015.00077 [cited 2022 Feb 7]. Available from:
Grubman, A., Choo, X.Y., Chew, G., Ouyang, J.F., Sun, G., Croft, N.P., et al., 2021 May 21. Transcriptional signature in microglia associated with Aβ plaque phagocytosis. Nat. Commun. 12 (1), 3015.
Guyon, A., Rousseau, J., Bégin, F.G., Bertin, T., Lamothe, G., Tremblay, J.P., 2021 Jun 4. Base editing strategy for insertion of the A673T mutation in the APP gene to prevent the development of AD in vitro. Mol. Ther. Nucleic Acids. (24), 253–263.
Guyon, A., Rousseau, J., Lamothe, G., Tremblay, J.P., 2020 Dec 28. The protective mutation A673T in amyloid precursor protein gene decreases Aβ peptides production for 14 forms of familial Alzheimer's disease in SH-SY5Y cells. PLoS One 15 (12), e0237122.
Haass, C., Lemere, C.A., Capell, A., Citron, M., Seubert, P., Schenk, D., et al., 1995 Dec. The Swedish mutation causes early-onset Alzheimer's disease by β-secretase cleavage within the secretory pathway. Nat. Med. 1 (12), 1291–1296.
Habib, A., Sawmiller, D., Tan, J., 2017. Restoring soluble amyloid precursor protein α functions as a potential treatment for Alzheimer's disease. J. Neurosci. Res. 95 (4), 973–991.
Hagmeyer, S., Romão, M.A., Cristóvão, J.S., Vilella, A., Zoli, M., Gomes, C.M., et al., 2019. Distribution and Relative Abundance of S100 Proteins in the Brain of the APP23 Alzheimer's Disease Model Mice. Front. Neurosci. 13 https://doi.org/10.3389/fnins.2019.00640. Available from:. [cited 2022 Jan 31].
Haldar, B., Hamilton, C.L., Solodushko, V., Abney, K.A., Alexeyev, M., Honkanen, R.E., et al., 2020 Feb. S100A6 is a positive regulator of PPP5C-FKBP51-dependent regulation of endothelial calcium signaling. FASEB J. 34 (2), 3179–3196.
Hamilton, R., Patel, S., Lee, E.B., Jackson, E.M., Lopinto, J., Arnold, S.E., et al., 2010 Oct. Lack of shunt response in suspected idiopathic Normal pressure hydrocephalus with Alzheimer disease pathology. Ann. Neurol. 68 (4), 535–540.
Hampel, H., Vassar, R., De Strooper, B., Hardy, J., Willem, M., Singh, N., et al., 2021 Apr 15. The β-secretase BACE1 in Alzheimer's disease. Biol. Psychiatry 89 (8), 745–756.
Hardy, J., Allsop, D., 1991 Jan 1. Amyloid deposition as the central event in the aetiology of Alzheimer's disease. Trends Pharmacol. Sci. (12), 383–388.
Harper, A.R., Nayee, S., Topol, E.J., 2015 Dec. Protective alleles and modifier variants in human health and disease. Nat. Rev. Genet. 16 (12), 689–701.
Heneka, M.T., Carson, M.J., Khoury, J.E., Landreth, G.E., Brosseron, F., Feinstein, D.L., et al., 2015 Apr 1. Neuroinflammation in Alzheimer's disease. The Lancet Neurology. 14 (4), 388–405.
Heslegrave, A., Heywood, W., Paterson, R., Magdalinou, N., Svensson, J., Johansson, P., et al., 2016 Jan 12. Increased cerebrospinal fluid soluble TREM2 concentration in Alzheimer's disease. Mol. Neurodegener. 11 (1), 3.
Hiltunen, M., Helisalmi, S., Mannermaa, A., Alafuzoff, I., Koivisto, A.M., Lehtovirta, M., et al., 2000 Apr. Identification of a novel 4.6-kb genomic deletion in presenilin-1 gene which results in exclusion of exon 9 in a Finnish early onset Alzheimer's disease family: an Alu core sequence-stimulated recombination? Eur. J. Hum. Genet. 8 (4), 259–266.
Hsiao, K., Chapman, P., Nilsen, S., Eckman, C., Harigaya, Y., Younkin, S., et al., 1996 Oct 4. Correlative memory deficits, Abeta elevation, and amyloid plaques in transgenic mice. Science. 274 (5284), 99–102.
Hu, Y.Y., He, S.S., Wang, X.C., Duan, Q.H., Khatoon, S., Iqbal, K., et al., 2002 Mar 8. Elevated levels of phosphorylated neurofilament proteins in cerebrospinal fluid of Alzheimer disease patients. Neurosci. Lett. 320 (3), 156–160.
Iwata, N., Tsubuki, S., Takaki, Y., Watanabe, K., Sekiguchi, M., Hosoki, E., et al., 2000 Feb. Identification of the major Abeta1-42-degrading catabolic pathway in brain parenchyma: suppression leads to biochemical and pathological deposition. Nat. Med. 6 (2), 143–150.
Jankowsky, J.L., Zheng, H., 2017 Dec 22. Practical considerations for choosing a mouse model of Alzheimer's disease. Mol. Neurodegener. 12 (1), 89.
Johnston, J.A., Cowburn, R.F., Norgren, S., Wiehager, B., Venizelos, N., Winblad, B., et al., 1994 Nov 14. Increased beta-amyloid release and levels of amyloid precursor protein (APP) in fibroblast cell lines from family members with the Swedish Alzheimer's disease APP670/671 mutation. FEBS Lett. 354 (3), 274–278.
Jonsson, T., Atwal, J.K., Steinberg, S., Snaedal, J., Jonsson, P.V., Bjornsson, S., et al., 2012 Aug 2. A mutation in APP protects against Alzheimer's disease and age-related cognitive decline. Nature. 488 (7409), 96–99.
Josse, J., Husson, F., 2016 Apr 4. missMDA: a package for handling missing values in multivariate data analysis. J. Stat. Softw. (70), 1–31.
Junkkari, A., Luikku, A.J., Danner, N., Jyrkkänen, H.K., Rauramaa, T., Korhonen, V.E., et al., 2019 Jul 25. The Kuopio idiopathic normal pressure hydrocephalus protocol: initial outcome of 175 patients. Fluids Barr. CNS. 16 (1), 21.
Käll, L., Canterbury, J.D., Weston, J., Noble, W.S., MacCoss, M.J., 2007 Nov. Semi-supervised learning for peptide identification from shotgun proteomics datasets. Nat. Methods 4 (11), 923–925.
Kero, M., Paetau, A., Polvikoski, T., Tanskanen, M., Sulkava, R., Jansson, L., et al., 2013 May 1. Amyloid precursor protein (APP) A673T mutation in the elderly Finnish population. Neurobiol. Aging 34 (5), 1518.e1–1518.e3.
Keshishian, H., Burgess, M.W., Specht, H., Wallace, L., Clauser, K.R., Gillette, M.A., et al., 2017 Aug. Quantitative, multiplexed workflow for deep analysis of human blood plasma and biomarker discovery by mass spectrometry. Nat. Protoc. 12 (8), 1683–1701.
Khani, M., Gibbons, E., Bras, J., Guerreiro, R., 2022 Jan 9. Challenge accepted: uncovering the role of rare genetic variants in Alzheimer's disease. Mol. Neurodegener. 17 (1), 3.
Kilańczyk, E., Graczyk, A., Ostrowska, H., Kasacka, I., Leśniak, W., Filipek, A., 2012 Jun 1. S100A6 is transcriptionally regulated by β-catenin and interacts with a novel target, Lamin a/C, in colorectal cancer cells. Cell Calcium 51 (6), 470–477.
Kim, Y.H., Choi, S.H., D'Avanzo, C., Hebisch, M., Sliwinski, C., Bylykbashi, E., et al., 2015 Jul. A 3D human neural cell culture system for modeling Alzheimer's disease. Nat. Protoc. 10 (7), 985–1006.
Kimura, A., Hata, S., Suzuki, T., 2016 Nov 11. Alternative selection of β-site APP-cleaving enzyme 1 (BACE1) cleavage sites in amyloid β-protein precursor (APP) harboring protective and pathogenic mutations within the Aβ sequence. J. Biol. Chem. 291 (46), 24041–24053.
Kokawa, A., Ishihara, S., Fujiwara, H., Nobuhara, M., Iwata, M., Ihara, Y., et al., 2015 Nov 4. The A673T mutation in the amyloid precursor protein reduces the production of β-amyloid protein from its β-carboxyl terminal fragment in cells. Acta Neuropathol Commun. (3), 66.
Kooistra, J., Milojevic, J., Melacini, G., Ortega, J., 2009. A new function of human HtrA2 as an amyloid-beta oligomerization inhibitor. J. Alzheimers Dis. 17 (2), 281–294.
Lai, X., Hu, J., Liu, H., Lan, L., Long, Y., Gao, X., et al., 2022 Jan 23. A short peptide from sAPPα binding to BACE1-APP action site rescues Alzheimer-like pathology. Neurosci. Lett. (770), 136397
Lannfelt, L., Basun, H., Wahlund, L.O., Rowe, B.A., Wagner, S.L., 1995 Aug. Decreased α-secretase-cleaved amyloid precursor protein as a diagnostic marker for Alzheimer's diseas. Nat. Med. 1 (8), 829–832.
Leinonen, V., Koivisto, A.M., Alafuzoff, I., Pyykkö, O.T., Rummukainen, J., von Und, Zu, Fraunberg, M., et al., 2012. Cortical brain biopsy in long-term prognostication of 468 patients with possible normal pressure hydrocephalus. Neurodegener. Dis. 10 (1–4), 166–169.
Leinonen, V., Koivisto, A.M., Savolainen, S., Rummukainen, J., Sutela, A., Vanninen, R., et al., 2012. Post-mortem findings in 10 patients with presumed normal-pressure hydrocephalus and review of the literature. Neuropathol. Appl. Neurobiol. 38 (1), 72–86.
Leinonen, V., Koivisto, A.M., Savolainen, S., Rummukainen, J., Tamminen, J.N., Tillgren, T., et al., 2010. Amyloid and tau proteins in cortical brain biopsy and Alzheimer's disease. Ann. Neurol. 68 (4), 446–453.
Levy-Lahad, E., Wasco, W., Poorkaj, P., Romano, D.M., Oshima, J., Pettingell, W.H., et al., 1995 Aug 18. Candidate gene for the chromosome 1 familial Alzheimer's disease locus. Science. 269 (5226), 973–977.
Li, H., Wang, B., Wang, Z., Guo, Q., Tabuchi, K., Hammer, R.E., et al., 2010 Oct 5. Soluble amyloid precursor protein (APP) regulates transthyretin and klotho gene expression without rescuing the essential function of APP. Proc. Natl. Acad. Sci. U. S. A. 107 (40), 17362–17367.
Li, B., Yamamori, H., Tatebayashi, Y., Shafit-Zagardo, B., Tanimukai, H., Chen, S., et al., 2008 Jan. Failure of neuronal maturation in Alzheimer disease dentate gyrus. J. Neuropathol. Exp. Neurol. 67 (1), 78–84.
Lichtenthaler, S.F., 2011 Jan. α-Secretase in Alzheimer's disease: molecular identity, regulation and therapeutic potential. J. Neurochem. 116 (1), 10–21.
Lichtenthaler, S.F., Dominguez, D., Westmeyer, G.G., Reiss, K., Haass, C., Saftig, P., et al., 2003 Dec 5. The cell adhesion protein P-selectin glycoprotein Ligand-1 is a substrate for the aspartyl protease BACE1*. J. Biol. Chem. 278 (49), 48713–48719.
Limegrover, C.S., LeVine III, H., Izzo, N.J., Yurko, R., Mozzoni, K., Rehak, C., et al., 2021. Alzheimer's protection effect of A673T mutation may be driven by lower Aβ oligomer binding affinity. J. Neurochem. 157 (4), 1316–1330.
Lin, T.W., Chang, C.F., Chang, Y.J., Liao, Y.H., Yu, H.M., Chen, Y.R., 2017 Mar 31. Alzheimer's amyloid-β A2T variant and its N-terminal peptides inhibit amyloid-β fibrillization and rescue the induced cytotoxicity. PLoS One 12 (3), e0174561.
Liu, Y.W., He, Y.H., Zhang, Y.X., Cai, W.W., Yang, L.Q., Xu, L.Y., et al., 2014 Apr. Absence of A673T variant in APP gene indicates an alternative protective mechanism contributing to longevity in Chinese individuals. Neurobiol. Aging 35 (4), 935.e11–12.
Luikku, A.J., Hall, A., Nerg, O., Koivisto, A.M., Hiltunen, M., Helisalmi, S., et al., 2019. Predicting development of Alzheimer's disease in patients with shunted idiopathic Normal pressure hydrocephalus. J. Alzheimers Dis. 71 (4), 1233–1243.

Maloney, J.A., Bainbridge, T., Gustafson, A., Zhang, S., Kyauk, R., Steiner, P., et al., 2014 Nov 7. Molecular mechanisms of Alzheimer disease protection by the A673T allele of amyloid precursor protein. J. Biol. Chem. 289 (45), 30990–31000.
Maloney, B., Lahiri, D.K., 2011 Nov 15. The Alzheimer's amyloid β-peptide (Aβ) binds a specific DNA Aβ-interacting domain (AβID) in the APP, BACE1, and APOE promoters in a sequence-specific manner: characterizing a new regulatory motif. Gene. 488 (1–2), 1–12.
Martin, L., Latypova, X., Wilson, C.M., Magnaudeix, A., Perrin, M.L., Terro, F., 2013 Jan 1. Tau protein phosphatases in Alzheimer's disease: the leading role of PP2A. Ageing Res. Rev. 12 (1), 39–49.
Martiskainen, H., Herukka, S.K., Stančáková, A., Paananen, J., Soininen, H., Kuusisto, J., et al., 2017. Decreased plasma β-amyloid in the Alzheimer's disease APP A673T variant carriers. Ann. Neurol. 82 (1), 128–132.
Marttinen, M., Paananen, J., Neme, A., Mitra, V., Takalo, M., Natunen, T., et al., 2019 Apr 1. A multiomic approach to characterize the temporal sequence in Alzheimer's disease-related pathology. Neurobiol. Dis. (124), 454–468.
Mehta, P.D., Pirttilä, T., Mehta, S.P., Sersen, E.A., Aisen, P.S., Wisniewski, H.M., 2000 Jan. Plasma and cerebrospinal fluid levels of amyloid beta proteins 1-40 and 1-42 in Alzheimer disease. Arch. Neurol. 57 (1), 100–105.
Mendsaikhan, A., Tooyama, I., Walker, D.G., 2019 Mar 11. Microglial Progranulin: involvement in Alzheimer's disease and neurodegenerative diseases. Cells. 8 (3), 230.
Moriya, M., Miyajima, M., Nakajima, M., Ogino, I., Arai, H., 2015. Impact of cerebrospinal fluid shunting for idiopathic normal pressure hydrocephalus on the amyloid cascade. PLoS One 10 (3), e0119973.
Multhaup, G., Huber, O., Buée, L., Galas, M.C., 2015 Sep 25. Amyloid precursor protein (APP) metabolites APP intracellular fragment (AICD), Aβ42, and tau in nuclear roles. J. Biol. Chem. 290 (39), 23515–23522.
Muratore, C.R., Rice, H.C., Srikanth, P., Callahan, D.G., Shin, T., Benjamin, L.N.P., et al., 2014 Jul 1. The familial Alzheimer's disease APPV717I mutation alters APP processing and tau expression in iPSC-derived neurons. Hum. Mol. Genet. 23 (13), 3523–3536.
Nasiri, E., Sankowski, R., Dietrich, H., Oikonomidi, A., Huerta, P.T., Popp, J., et al., 2020 Apr 17. Key role of MIF-related neuroinflammation in neurodegeneration and cognitive impairment in Alzheimer's disease. Mol. Med. 26 (1), 34.
Obregon, D., Hou, H., Deng, J., Giunta, B., Tian, J., Darlington, D., et al., 2012 Apr 10. Soluble amyloid precursor protein-α modulates β-secretase activity and amyloid-β generation. Nat. Commun. 3 (1), 777.
Palmqvist, S., Insel, P.S., Stomrud, E., Janelidze, S., Zetterberg, H., Brix, B., et al., 2019 Dec. Cerebrospinal fluid and plasma biomarker trajectories with increasing amyloid deposition in Alzheimer's disease. EMBO Mol Med. 11 (12), e11170.
Panyard, D.J., Kim, K.M., Darst, B.F., Deming, Y.K., Zhong, X., Wu, Y., et al., 2021 Jan 12. Cerebrospinal fluid metabolomics identifies 19 brain-related phenotype associations. Commun Biol. 4 (1), 1–11.
Perluigi, M., Barone, E., Di Domenico, F., Butterfield, D.A., 2016 Oct 1. Aberrant protein phosphorylation in Alzheimer disease brain disturbs pro-survival and cell death pathways. Biochim. Biophys. Acta (BBA) - Mol. Basis Dis. 1862 (10), 1871–1882.
Peters-Libeu, C., Campagna, J., Mitsumori, M., Poksay, K.S., Spilman, P., Sabogal, A., et al., 2015 Jan 1. sAβPP α is a potent endogenous inhibitor of BACE1. J. Alzheimers Dis. 47 (3), 545–555.
Prausmüller, S., Arfsten, H., Spinka, G., Freitag, C., Bartko, P.E., Goliasch, G., et al., 2020 Jun 2. Plasma Neprilysin displays no relevant association with Neurohumoral activation in chronic HFrEF. J. Am. Heart Assoc. 9 (11), e015071.
Prihar, G., Verkkoniem, A., Perez-Tur, J., Crook, R., Lincoln, S., Houlden, H., et al., 1999 Oct. Alzheimer disease PS-1 exon 9 deletion defined. Nat. Med. 5 (10), 1090.
Rauramaa, T., Pikkarainen, M., Englund, E., Ince, P.G., Jellinger, K., Paetau, A., et al., 2013 Jun 1. Consensus recommendations on pathologic changes in the Hippocampus: a postmortem multicenter inter-rater study. J. Neuropathol. Exp. Neurol. 72 (6), 452–461.
Ridge, P.G., Mukherjee, S., Crane, P.K., Kauwe, J.S.K., 2013. Alzheimer's disease genetics consortium. Alzheimer's disease: analyzing the missing heritability. PLoS One 8 (11), e79771.
Ritchie, M.E., Phipson, B., Wu, D., Hu, Y., Law, C.W., Shi, W., et al., 2015 Apr 20. Limma powers differential expression analyses for RNA-sequencing and microarray studies. Nucleic Acids Res. 43 (7), e47.
Ryan, M.M., Morris, G.P., Mockett, B.G., Bourne, K., Abraham, W.C., Tate, W.P., et al., 2013 Jun 6. Time-dependent changes in gene expression induced by secreted amyloid precursor protein-alpha in the rat hippocampus. BMC Genomics 14 (1), 376.
Savage, M.J., Holder, D.J., Wu, G., Kaplow, J., Siuciak, J.A., Potter, W.Z., et al., 2015 Jan 1. Soluble BACE-1 activity and sAβPPβ concentrations in Alzheimer's disease and age-matched healthy control cerebrospinal fluid from the Alzheimer's disease neuroimaging Initiative-1 baseline cohort. J. Alzheimers Dis. 46 (2), 431–440.
Schettini, G., Govoni, S., Racchi, M., Rodriguez, G., 2010. Phosphorylation of APP-CTF-AICD domains and interaction with adaptor proteins: signal transduction and/or transcriptional role – relevance for Alzheimer pathology. J. Neurochem. 115 (6), 1299–1308.
Selkoe, D.J., 1998 Nov. The cell biology of beta-amyloid precursor protein and presenilin in Alzheimer's disease. Trends Cell Biol. 8 (11), 447–453.
Seppala, T.T., Nerg, O., Koivisto, A.M., Rummukainen, J., Puli, L., Zetterberg, H., et al., 2012 May 15. CSF biomarkers for Alzheimer disease correlate with cortical brain biopsy findings. Neurology. 78 (20), 1568–1575.
Shankar, G.M., Walsh, D.M., 2009 Nov 23. Alzheimer's disease: synaptic dysfunction and Aβ. Mol. Neurodegener. 4 (1), 48.
Shastry, B.S., Giblin, F.J., 1999 Jan 15. Genes and susceptible loci of Alzheimer's disease. Brain Res. Bull. 48 (2), 121–127.
Sherrington, R., Rogaev, E.I., Liang, Y., Rogaeva, E.A., Levesque, G., Ikeda, M., et al., 1995 Jun 29. Cloning of a gene bearing missense mutations in early-onset familial Alzheimer's disease. Nature. 375 (6534), 754–760.
Słomnicki, L.P., Leśniak, W., 2008. A putative role of the amyloid precursor protein intracellular domain (AICD) in transcription. Acta Neurobiol. Exp. (Wars) 68 (2), 219–228.
Sobue, A., Komine, O., Hara, Y., Endo, F., Mizoguchi, H., Watanabe, S., et al., 2021 Jan 5. Microglial gene signature reveals loss of homeostatic microglia associated with neurodegeneration of Alzheimer's disease. Acta Neuropathologica Communicat. 9 (1), 1.
Stancáková, A., Javorský, M., Kuulasmaa, T., Haffner, S.M., Kuusisto, J., Laakso, M., 2009 May. Changes in insulin sensitivity and insulin release in relation to glycemia and glucose tolerance in 6,414 Finnish men. Diabetes. 58 (5), 1212–1221.
Steiner, H., Romig, H., Grim, M.G., Philipp, U., Pesold, B., Citron, M., et al., 1999 Mar 19. The biological and pathological function of the presenilin-1 Deltaexon 9 mutation is independent of its defect to undergo proteolytic processing. J. Biol. Chem. 274 (12), 7615–7618.
Strittmatter, W.J., Saunders, A.M., Schmechel, D., Pericak-Vance, M., Enghild, J., Salvesen, G.S., et al., 1993 Mar 1. Apolipoprotein E: high-avidity binding to beta-amyloid and increased frequency of type 4 allele in late-onset familial Alzheimer disease. Proc. Natl. Acad. Sci. U. S. A. 90 (5), 1977–1981.
Su, D., Su, Z., Wang, J., Yang, S., Ma, J., 2009. UCF-101, a novel Omi/HtrA2 inhibitor, protects against cerebral ischemia/reperfusion injury in rats. Anat. Rec. 292 (6), 854–861.
Suárez-Calvet, M., Capell, A., Araque Caballero, M.Á., Morenas-Rodríguez, E., Fellerer, K., Franzmeier, N., et al., 2018 Dec. CSF progranulin increases in the course of Alzheimer's disease and is associated with sTREM2, neurodegeneration and cognitive decline. EMBO Mol Med. 10 (12), e9712.
Suk, K., 2010 Apr. Combined analysis of the glia secretome and the CSF proteome: neuroinflammation and novel biomarkers. Expert Rev Proteom. 7 (2), 263–274.
Suzuki, N., Cheung, T.T., Cai, X.D., Odaka, A., Otvos, L., Eckman, C., et al., 1994 May 27. An increased percentage of long amyloid beta protein secreted by familial amyloid beta protein precursor (beta APP717) mutants. Science. 264 (5163), 1336–1340.
Tambini, M.D., Yao, W., D'Adamio, L., 2019 Dec. Facilitation of glutamate, but not GABA, release in familial Alzheimer's APP mutant Knock-in rats with increased β-cleavage of APP. Aging Cell 18 (6), e13033.
Taus, T., Köcher, T., Pichler, P., Paschke, C., Schmidt, A., Henrich, C., et al., 2011 Dec 2. Universal and confident phosphorylation site localization using phosphoRS. J. Proteome Res. 10 (12), 5354–5362.
Thordardottir, S., Kinhult Ståhlbom, A., Almkvist, O., Thonberg, H., Eriksdotter, M., Zetterberg, H., et al., 2017 Feb 16. The effects of different familial Alzheimer's disease mutations on APP processing in vivo. Alzheimers Res. Ther. 9 (1), 9.
Tian, Y., Crump, C.J., Li, Y.M., 2010 Oct 15. Dual role of alpha-secretase cleavage in the regulation of gamma-secretase activity for amyloid production. J. Biol. Chem. 285 (42), 32549–32556.
Tian, Q., Lin, Z.Q., Wang, X.C., Chen, J., Wang, Q., Gong, C.X., et al., 2004 Jan 1. Injection of okadaic acid into the meynert nucleus basalis of rat brain induces decreased acetylcholine level and spatial memory deficit. Neuroscience. 126 (2), 277–284.
Torretta, E., Arosio, B., Barbacini, P., Capitanio, D., Rossi, P.D., Moriggi, M., et al., 2021 Jan. Novel insight in idiopathic Normal pressure hydrocephalus (iNPH) biomarker discovery in CSF. Int. J. Mol. Sci. 22 (15), 8034.
Tsukamoto, K., Watanabe, T., Matsushima, T., Kinoshita, M., Kato, H., Hashimoto, Z., et al., 1993. Apr. Determination by PCR-RFLP of apo E genotype in a Japanese population. J. Lab. Clin. Med. 121 (4) [cited 2022 Jan 18]. Available from. https://pubmed.ncbi.nlm.nih.gov/8095964/ [cited 2022 Jan 18]. Available from.
Wang, J.Z., Grundke-Iqbal, I., Iqbal, K., 1996 Jun 1. Restoration of biological activity of Alzheimer abnormally phosphorylated τ by dephosphorylation with protein phosphatase-2A, −2B and −1. Mol. Brain Res. 38 (2), 200–208.
Wang, L.S., Naj, A.C., Graham, R.R., Crane, P.K., Kunkle, B.W., Cruchaga, C., et al., 2015 Feb 1. Rarity of the Alzheimer Disease–Protective APP A673T Variant in the United States. JAMA Neurol. 72 (2), 209–216.
Wang, H., wei, Zhu X li, Qin L ming, Qian H jun, Wang Y., 2015 Jan 1. Microglia activity modulated by T cell Ig and mucin domain protein 3 (Tim-3). Cell. Immunol. 293 (1), 49–58.
Westerlund, M., Behbahani, H., Gellhaar, S., Forsell, C., Belin, A.C., Anvret, A., et al., 2011. Altered enzymatic activity and allele frequency of OMI/HTRA2 in Alzheimer's disease. FASEB J. 25 (4), 1345–1352.
Wightman, D.P., Jansen, I.E., Savage, J.E., Shadrin, A.A., Bahrami, S., Holland, D., et al., 2021 Sep. A genome-wide association study with 1,126,563 individuals identifies new risk loci for Alzheimer's disease. Nat. Genet. 53 (9), 1276–1282.
Wruck, W., Schröter, F., Adjaye, J., 2016 Jan 1. Meta-analysis of transcriptome data related to Hippocampus biopsies and iPSC-derived neuronal cells from Alzheimer's disease patients reveals an association with FOXA1 and FOXA2 gene regulatory networks. J. Alzheimers Dis. 50 (4), 1065–1082.
Xu, X., 2009 Jan 1. γ-Secretase catalyzes sequential cleavages of the AβPP transmembrane domain. J. Alzheimers Dis. 16 (2), 211–224.
Yuan, A., Nixon, R.A., 2021. Neurofilament proteins as biomarkers to monitor neurological diseases and the efficacy of therapies. Front. Neurosci. 15, 1242.

Zhang, N., Parr, C.J.C., Birch, A.M., Goldfinger, M.H., Sastre, M., 2018 Oct 15. The amyloid precursor protein binds to β-catenin and modulates its cellular distribution. Neurosci. Lett. (685), 190–195.
Zhang, L., Trushin, S., Christensen, T.A., Tripathi, U., Hong, C., Geroux, R.E., et al., 2018 Jun. Differential effect of amyloid beta peptides on mitochondrial axonal trafficking depends on their state of aggregation and binding to the plasma membrane. Neurobiol. Dis. 114, 1–16.
Zhao, J., Liu, X., Xia, W., Zhang, Y., Wang, C., 2020. Targeting amyloidogenic processing of APP in Alzheimer's Disease. Fronti. Mol. Neurosci. 13 [cited 2022 Feb 1]. Available from: https://doi.org/10.3389/fnmol.2020.00137 [cited 2022 Feb 1]. Available from: